nature biomedical engineering

Supplementary information https://doi.org/10.1038/s41551-023-01032-2

# Peptide-mediated delivery of CRISPR enzymes for the efficient editing of primary human lymphocytes

**Contents**

**Supplementary figures**



**Supplementary tables**

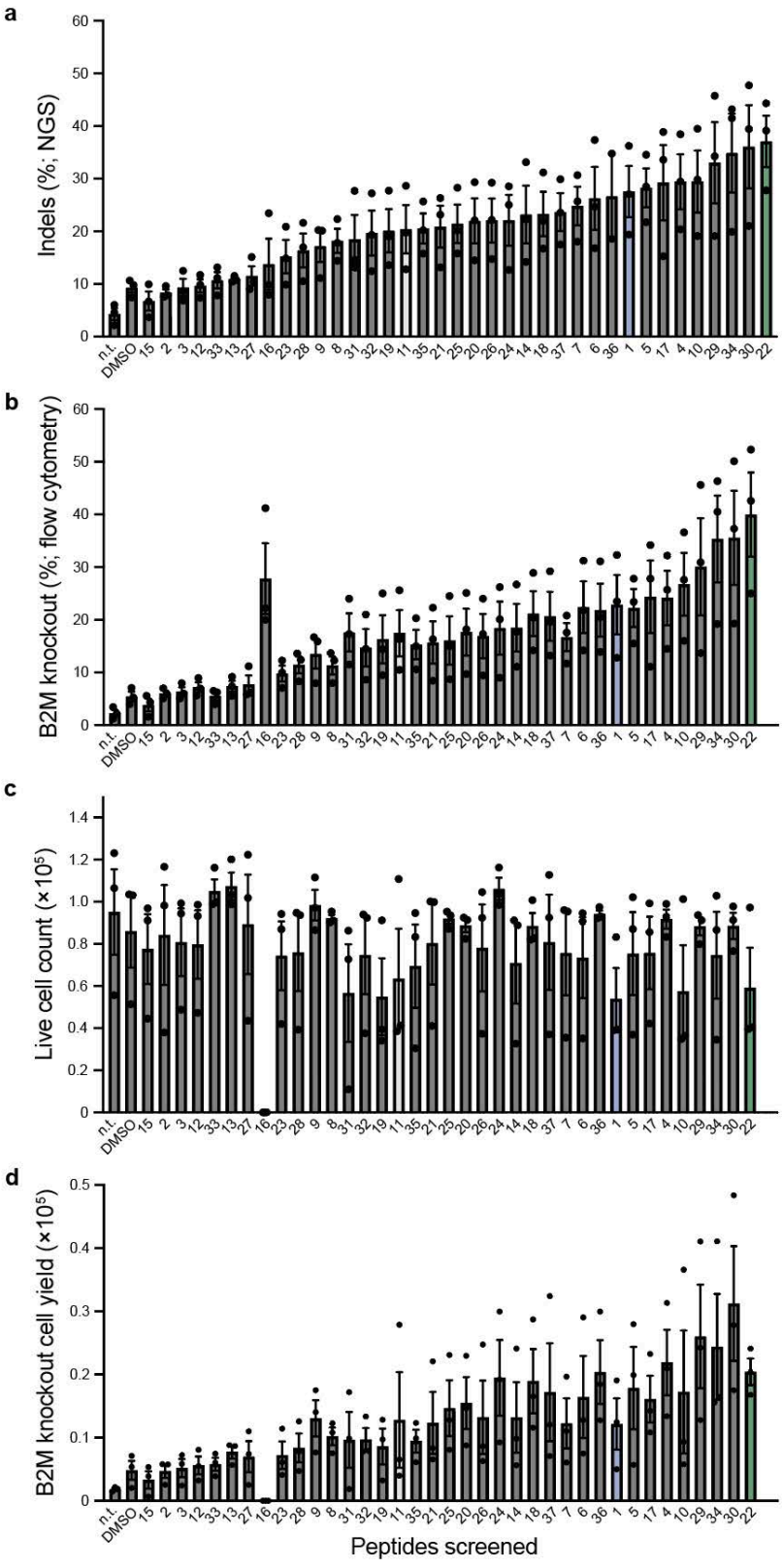


**Supplementary Fig. 1 |** Arrayed screening of 37 peptides for Cas9 RNP delivery. The bars in blue (#1, E5-TAT), light gray (#11, INF7-TAT), or green (#22, A5K) correspond to colors in **Supplementary Table 1**, and represent the peptides also tested in **Fig. 1c**. Peptides were evaluated three days after *B2M*-Cas9 RNP delivery to CD4⁺ T cells on the basis of **a**, indels produced at the *B2M* locus assessed by amplicon-based NGS (with efficiency being used to sort the peptides, an order maintained for the other plots), **b**, knockout of B2M surface expression assessed by flow cytometry, **c**, viability of cells evaluated by staining for dead cells with GhostDye780, and **d**, comparison of edited cell yield. Few cells survived PERC using the lysine-rich peptide 16, which likely underlies the incongruity between NGS and flow results (i.e. relative ranking).

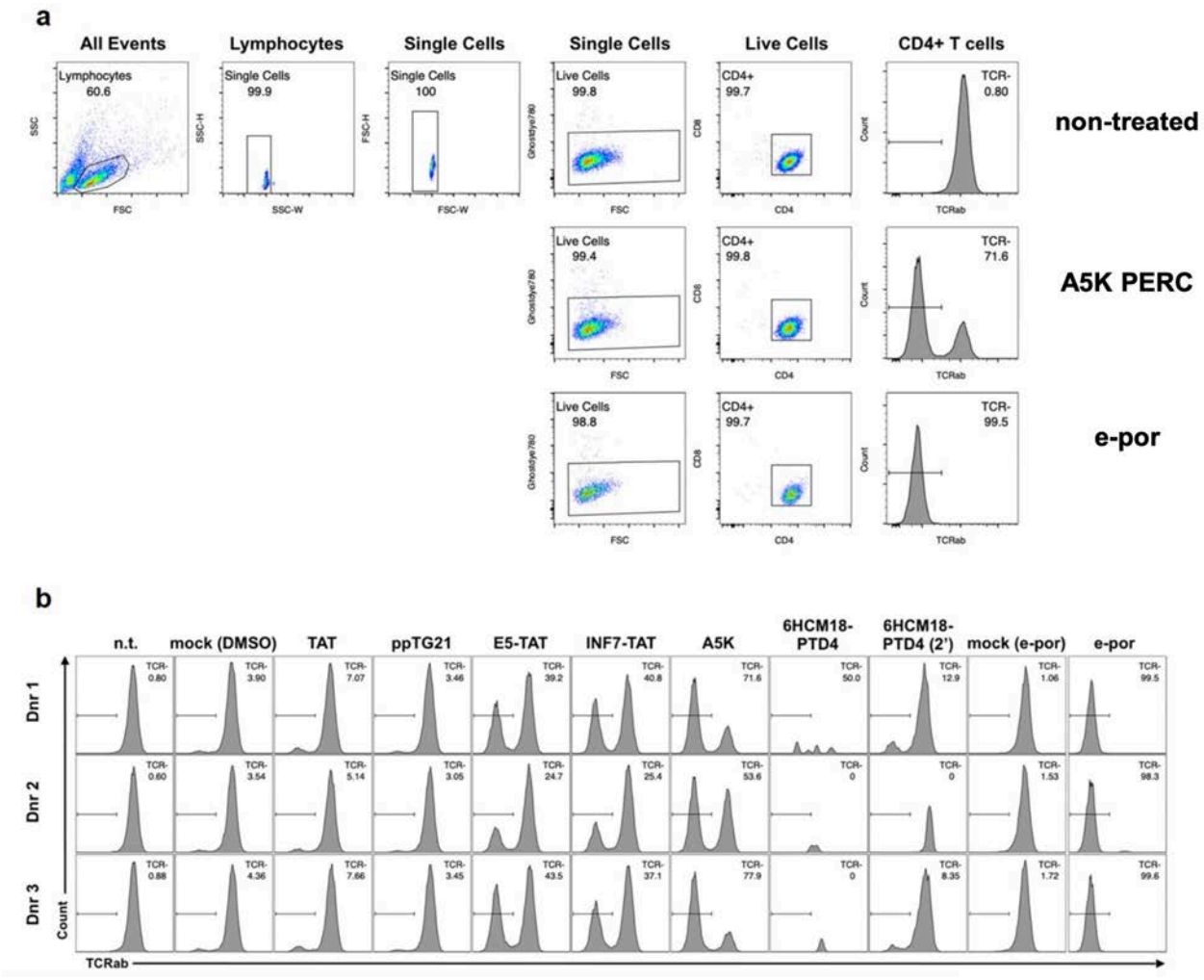


**Supplementary Fig. 2 | a**, Representative flow cytometry gating to assess knockout of TCR surface expression in CD4⁺ T cells. Data are related to **Fig. 1c**. **b**, Cas9 *TRAC*-RNP was delivered using various peptides or electroporation. Negative controls: mock peptide (DMSO only), mock electroporation, and non-treated (n.t.). Dnr = donor.

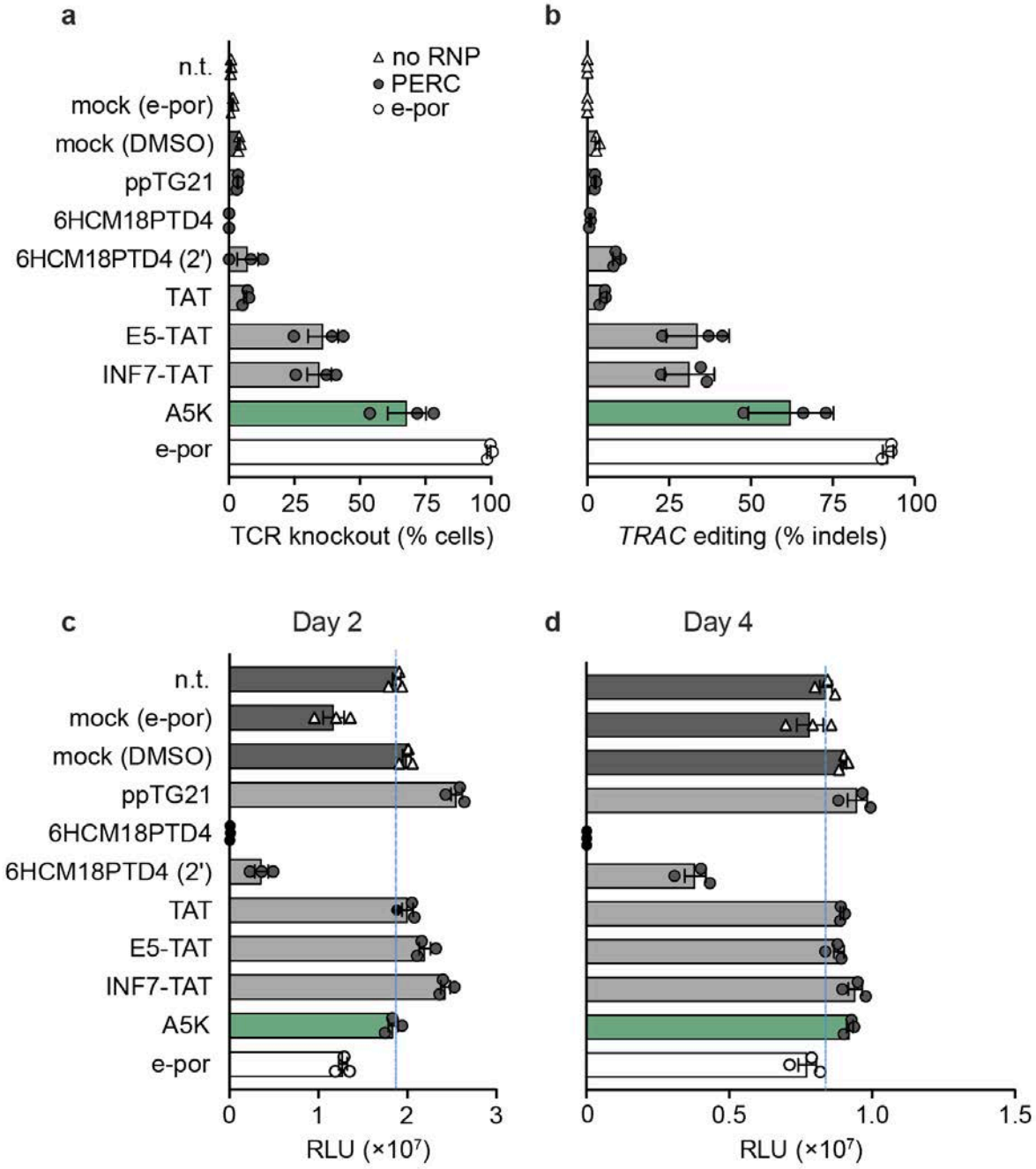


**Supplementary Fig. 3 |** Peptide-enabled Cas9 *TRAC*-RNP delivery to CD4⁺ T cells. Peptides' capacity for delivery was assessed based on **a**, flow cytometry for loss of TCR surface expression (also in **Fig. 1c**) and **b**, NGS for indels at the *TRAC* locus. **c,d**, Cell viability assay at **c**, two days after treatment (also in **Fig. 1c**) and **d**, four days after treatment. 2′ = two-minute treatment and subsequent wash; all other treatments remained on cells. n.t. = non-treated, mock = DMSO only, or electroporated (no RNP). n=3 biological replicates from distinct human donors. Bars represent mean, and error bars represent ± S.E.M.

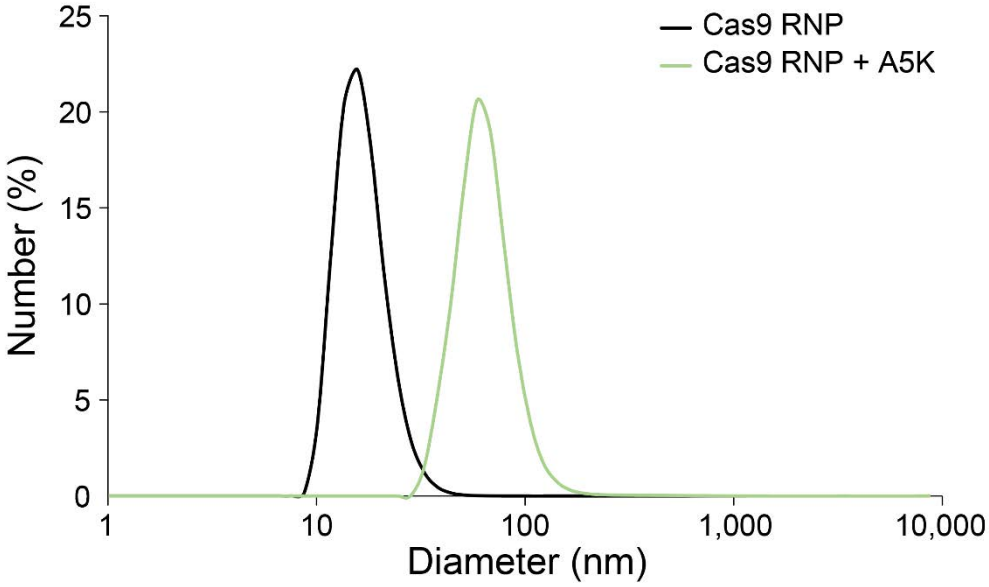


**Supplementary Fig. 4 |** Dynamic light scattering analysis. The analysis (performed “by number”) is of Cas9 *B2M*-RNP with and without the addition of A5K peptide in DMSO (1% v/v DMSO final). RNP alone is primarily ~20 nm particles: approximately the diameter expected based on prior 3D structures of CRISPR-Cas9 (~15 nm). In the presence of A5K peptide, ~60 nm particles are observed, most with a diameter <100 nm.

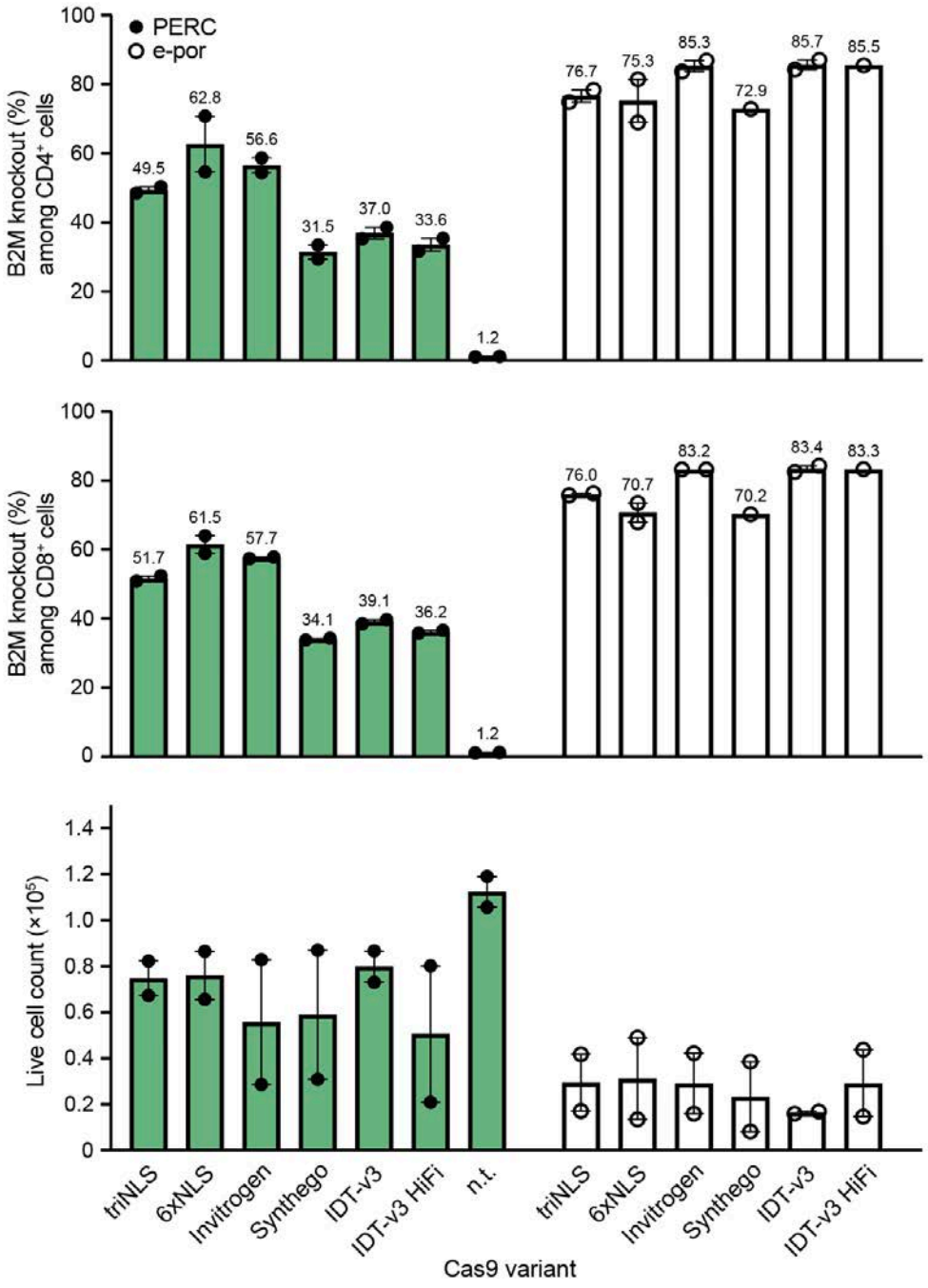


**Supplementary Fig. 5 |** Editing efficiency and viability following PERC or electroporation of various Cas9 enzymes. Two published NLS-rich constructs, triNLS and 6×NLS, were purified in academic labs (**Methods**). 6×NLS Cas9 was used in all other Cas9 nuclease experiments in this study. The other four constructs are from commercial vendors. Invitrogen: Invitrogen TrueCut Cas9 Protein v2 (ThermoFisher). Synthego: SpCas9 2NLS (Synthego). IDT-v3: Alt-R S.p. Cas9 Nuclease V3 (IDT). IDT-v3 HiFi: Alt-R S.p. HiFi Cas9 Nuclease V3 (IDT). n=2 biological replicates from distinct human donors. Bars represent mean, and error bars represent ± S.E.M.

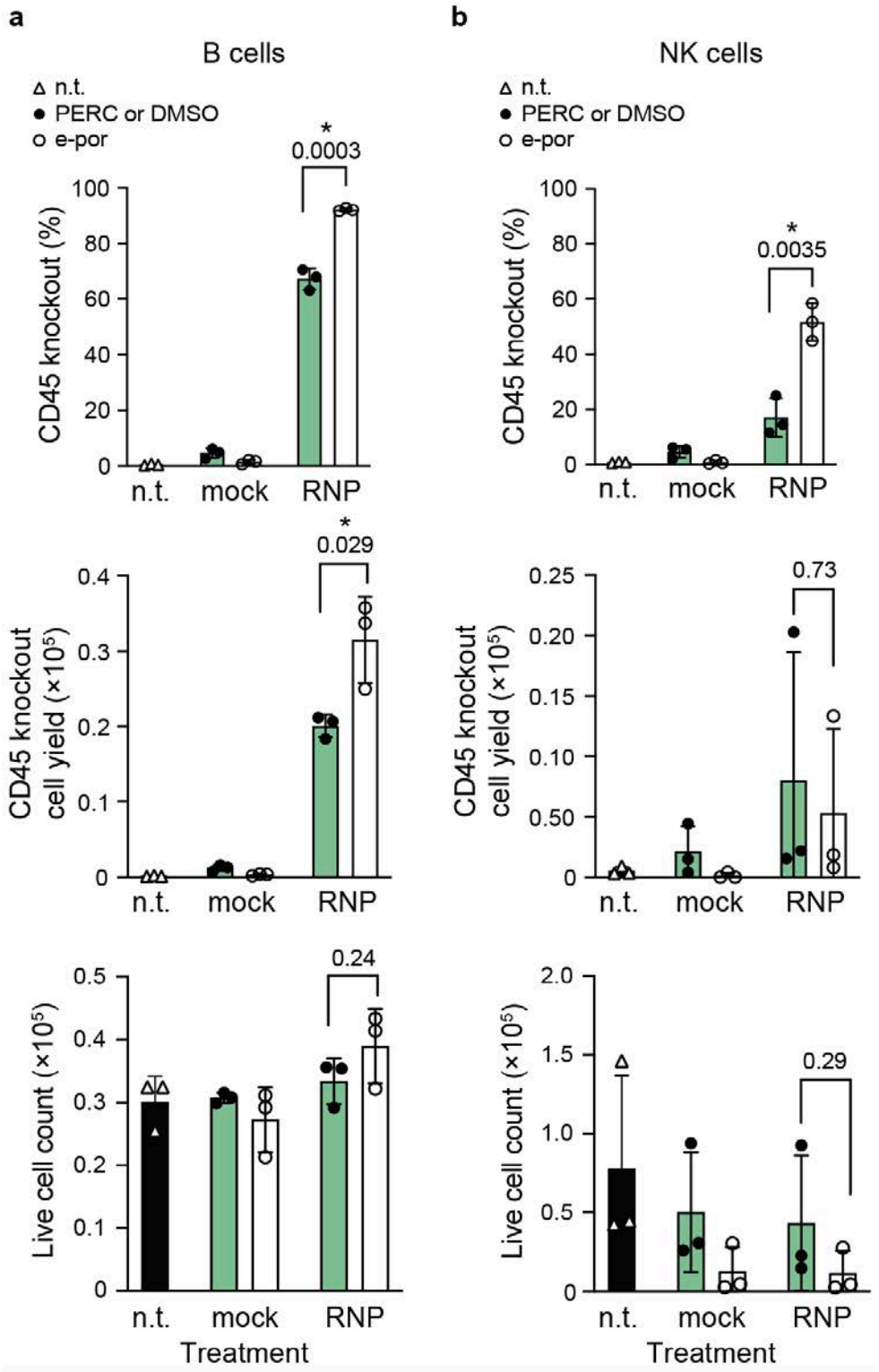


**Supplementary Fig. 6 |** PERC in primary human B cells and primary human NK cells. Peptide-enabled Cas9 *CD45*-RNP delivery to **a**, B cells and **b**, NK cells as measured by flow cytometry for CD45 surface expression. Results are presented as knockout frequency, edited cell yield, and total live cell count (independent of editing outcome). n=3 biological replicates from distinct human donors. Bars represent mean. Error bars represent S.D. *P*-values are from two-tailed unpaired *t*-tests with Holm-Sidak's correction method for multiple comparisons.

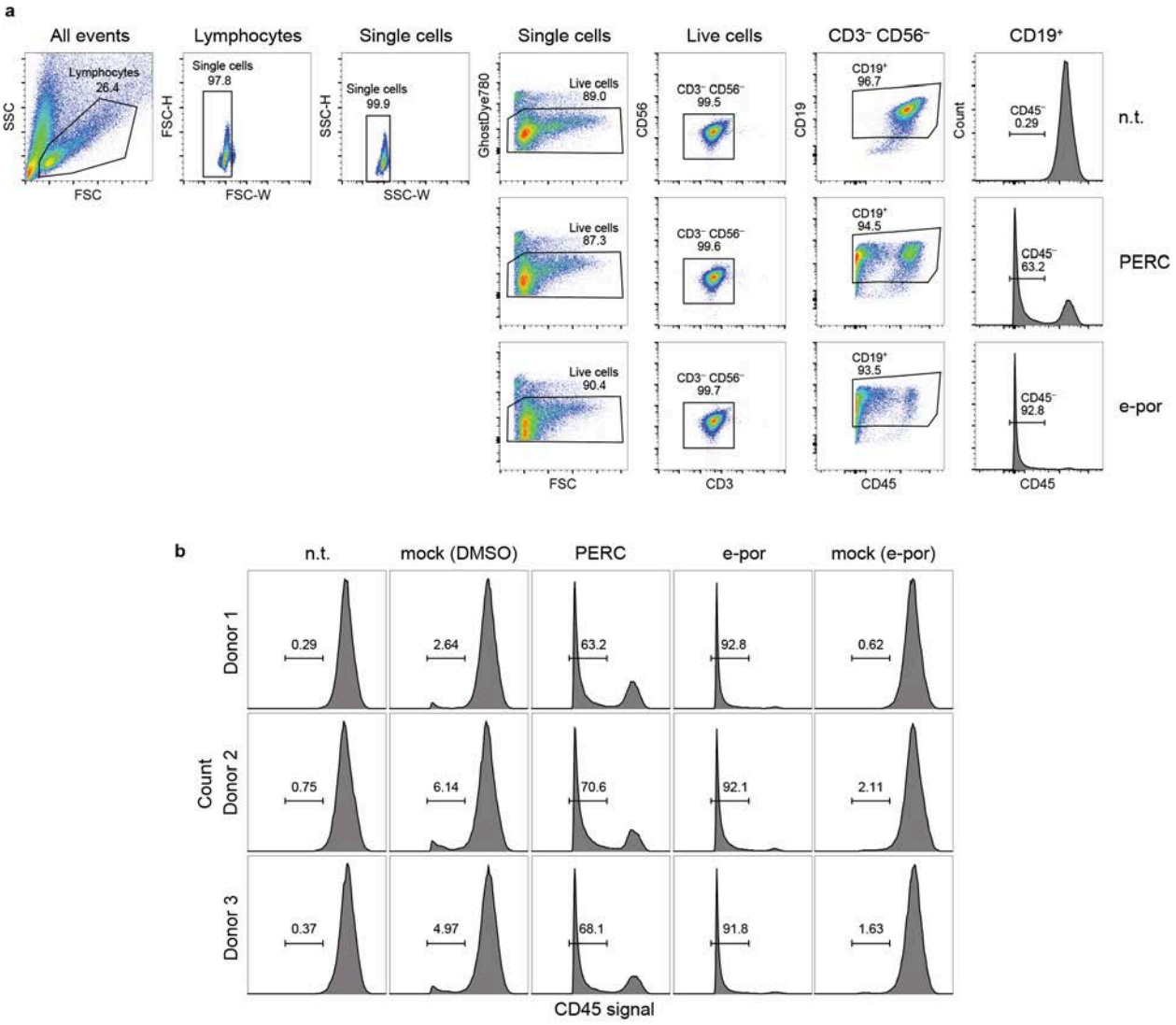


**Supplementary Fig. 7 | a**, Representative flow cytometry gating for assessing knockout of CD45 surface expression in B cells (related to **Supplementary Fig. 6a**). **b**, Cas9 *CD45*-RNP was delivered via PERC or electroporation (e-por), and frequencies of CD45 KO were assessed and compared to mock peptide (DMSO-treated), mock electroporated, and non-treated (n.t.) cells.

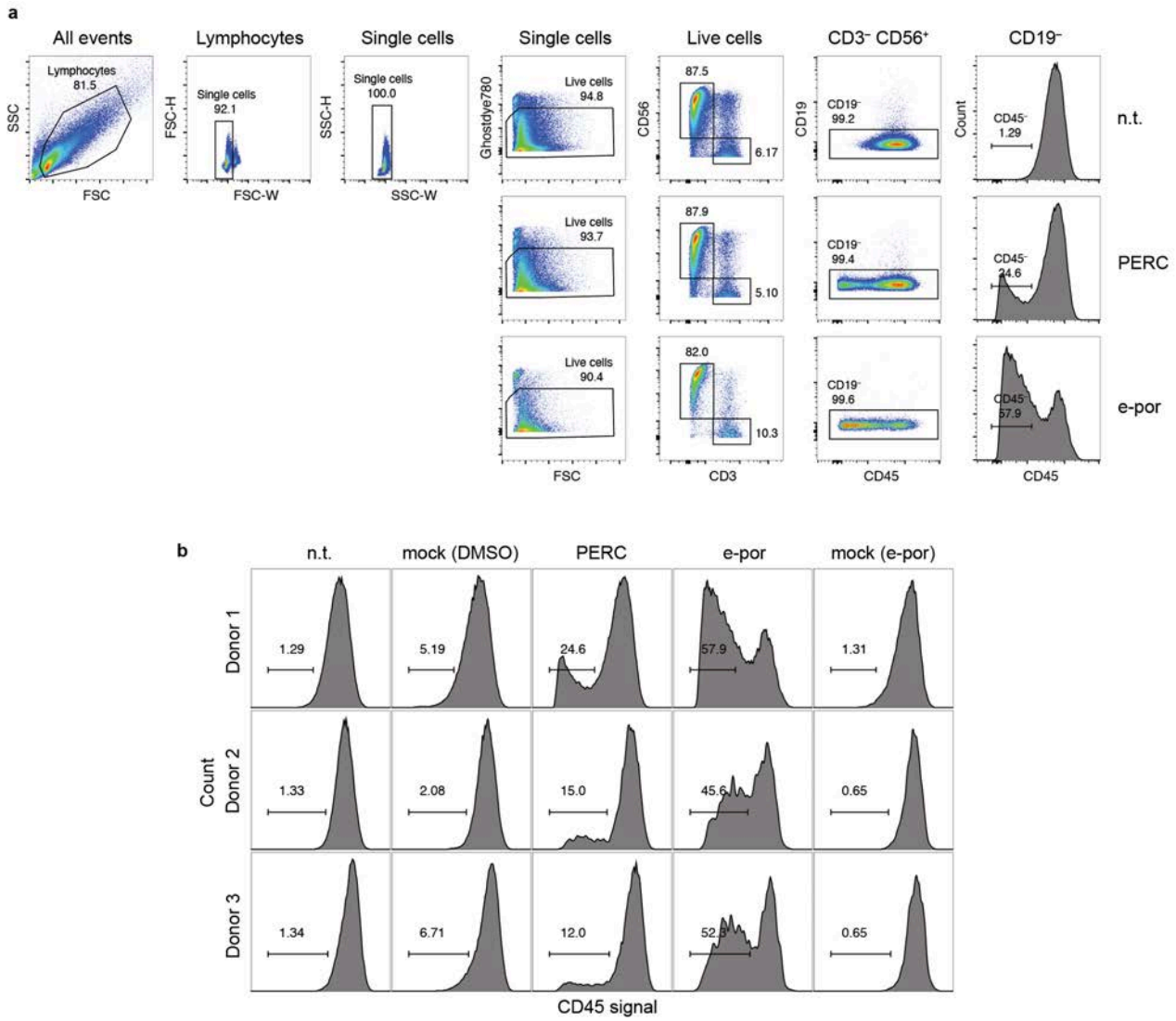


**Supplementary Fig. 8 | a**, Representative flow cytometry gating for assessing knockout of CD45 surface expression in NK cells (related to **Supplementary Fig. 6b**). **b**, Cas9 *CD45*-RNP was delivered via PERC or electroporation (e-por), and frequencies of CD45 KO were assessed and compared to mock peptide (DMSO-treated), mock electroporated, and non-treated (n.t.) cells.

**ABE8e-SpCas9-NG** dTadA/TadA8e dimer w/ C-term BP-SV40/Nuc 207362 Da

MKRTADGSEFESPKKKRKVSEVEFSHEYWMRHALTLAKRAWDEREVPVGAVLVHNNRVIGEGWNRPIGRHDPTAHA**A**IMAL
RQGGLVMQNYRLIDATLYVTLEPCVMCAGAMIHSRIGRVVFGARDAKTGAAGSLMDVLHHPGMNHRVEITEGILADECAAL
LSDFFRMRRQEIKAQKKAQSSTDSGGSSGGSSGSETPGTSESATPESSGGSSGGSSEVEFSHEYWMRHALTLAKRARDERE
VPVGAVLVLNNRVIGEGWNRAIGLHDPTAHAEIMALRQGGLVMQNYRLIDATLYVTFEPCVMCAGAMIHSRIGRVVFGVRN
SKRGAAGSLMNVLNYPGMNHRVEITEGILADECAALLCDFYRMPRQVFNAQKKAQSSINSGGSSGGSSGSETPGTSESATP
ESSGGSSGGSDKKYSIGL**A**IGTNSVGWAVITDEYKVPSKKFKVLGNTDRHSIKKNLIGALLFDSGETAEATRLKRTARRRY
TRRKNRICYLQEIFSNEMAKVDDSFFHRLEESFLVEEDKKHERHPIFGNIVDEVAYHEKYPTIYHLRKKLVDSTDKADLRL
IYLALAHMIKFRGHFLIEGDLNPDNSDVDKLFIQLVQTYNQLFEENPINASGVDAKAILSARLSKSRRLENLIAQLPGEKK
NGLFGNLIALSLGLTPNFKSNFDLAEDAKLQLSKDTYDDDLDNLLAQIGDQYADLFLAAKNLSDAILLSDILRVNTEITKA
PLSASMIKRYDEHHQDLTLLKALVRQQLPEKYKEIFFDQSKNGYAGYIDGGASQEEFYKFIKPILEKMDGTEELLVKLNRE
DLLRKQRTFDNGSIPHQIHLGELHAILRRQEDFYPFLKDNREKIEKILTFRIPYYVGPLARGNSRFAWMTRKSEETITPWN
FEEVVDKGASAQSFIERMTNFDKNLPNEKVLPKHSLLYEYFTVYNELTKVKYVTEGMRKPAFLSGEQKKAIVDLLFKTNRK
VTVKQLKEDYFKKIECFDSVEISGVEDRFNASLGTYHDLLKIIKDKDFLDNEENEDILEDIVLTLTLFEDREMIEERLKTY
AHLFDDKVMKQLKRRRYTGWGRLSRKLINGIRDKQSGKTILDFLKSDGFANRNFMQLIHDDSLTFKEDIQKAQVSGQGDSL
HEHIANLAGSPAIKKGILQTVKVVDELVKVMGRHKPENIVIEMARENQTTQKGQKNSRERMKRIEEGIKELGSQILKEHPV
ENTQLQNEKLYLYYLQNGRDMYVDQELDINRLSDYDVDHIVPQSFLKDDSIDNKVLTRSDKNRGKSDNVPSEEVVKKMKNY
WRQLLNAKLITQRKFDNLTKAERGGLSELDKAGFIKRQLVETRQITKHVAQILDSRMNTKYDENDKLIREVKVITLKSKLV
SDFRKDFQFYKVREINNYHHAHDAYLNAVVGTALIKKYPKLESEFVYGDYKVYDVRKMIAKSEQEIGKATAKYFFYSNIMN
FFKTEITLANGEIRKRPLIETNGETGEIVWDKGRDFATVRKVLSMPQVNIVKKTEVQTGGFSKESIRPKRNSDKLIARKKD
WDPKKYGGFVSPTVAYSVLVVAKVEKGKSKKLKSVKELLGITIMERSSFEKNPIDFLEAKGYKEVKKDLIIKLPKYSLFEL
ENGRKRMLASARFLQKGNELALPSKYVNFLYLASHYEKLKGSPEDNEQKQLFVEQHKHYLDEIIEQISEFSKRVILADANL
DKVLSAYNKHRDKPIREQAENIIHLFTLTNLGAPRAFKYFDTTIDRKVYRSTKEVLDATLIHQSITGLYETRIDLSQLGGD
SGGS**KRTADGSEFEPKKKRKV**GSGS**KRPAATKKAGQAKKKK**

**Supplementary Fig. 9 |** Amino acid sequence of the ABE8e-SpCas9-NG adenine base editor. Each TadA domain is in cyan; inactivating alanine mutations for the N-terminal TadA domain and for one nuclease domain of Cas9 are in bold; bipartite SV40 NLS is in purple; nucleoplasmin NLS is in dark blue.

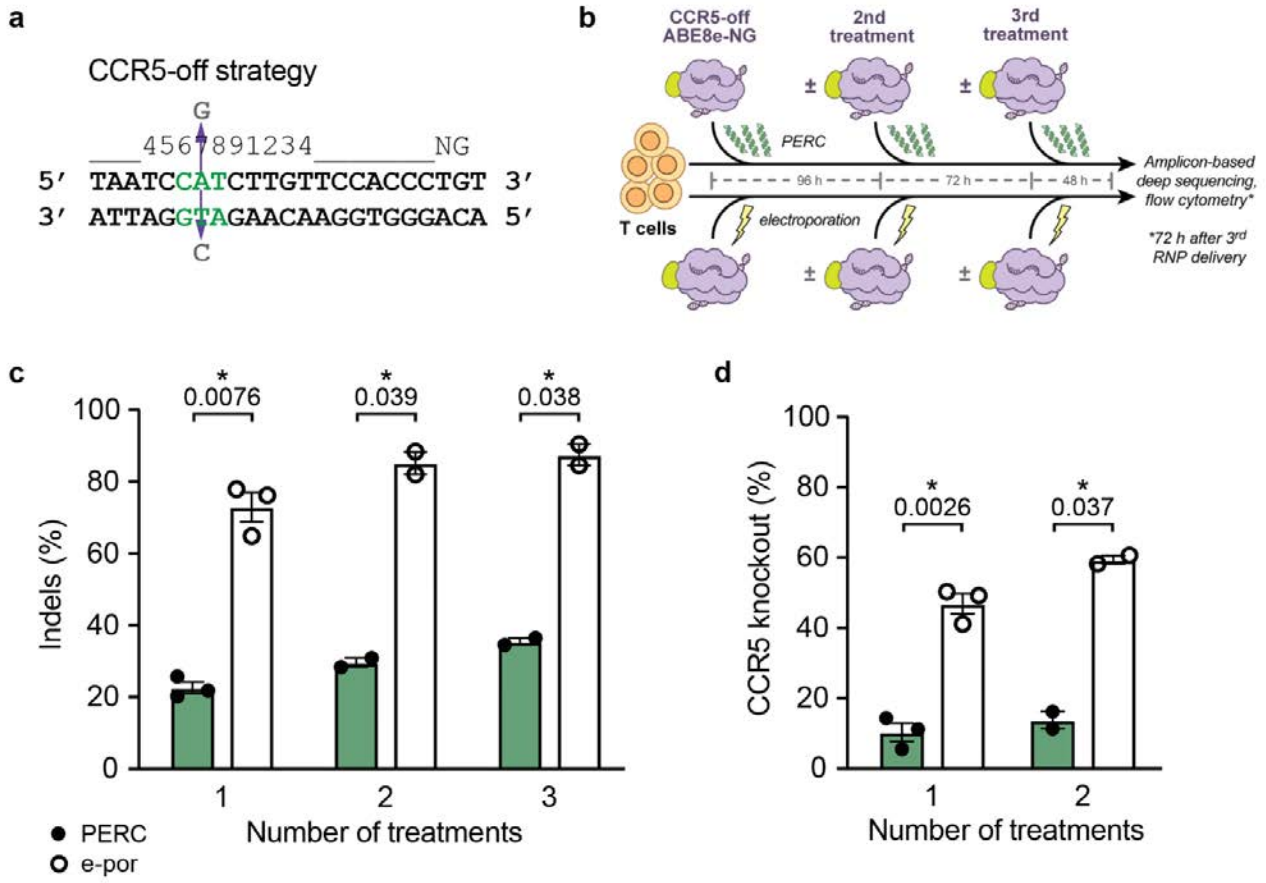


**Supplementary Fig. 10 |** Peptide-enabled base editor RNP delivery to T cells to abrogate the start codon of *CCR5*. **a**, Schematic for the base editing strategy. The spacer sequence is denoted by underscores, except for positions 4–14, which are represented by numerals to indicate the window of likely A-to-G base editing activity (shown as a red curve in the next two figures). The NG PAM is indicated to the right (3′ side) of the spacer sequence and was used because there are no proximal canonical NGG PAM sites. Purple arrows indicate changes induced by ABE activity, which eliminates the start codon ATG (green, bottom strand). This strategy was shown to be capable of knocking out of CCR5 surface expression in T cells (Knipping, et al. *Molecular Therapy* 2022). **b**, ABE8e-Cas9-NG base editor RNP was delivered via PERC or electroporation to human $CD4^+$ T cells. Cells were treated with a single dose or treated sequentially two or three times, with 3–4 days between treatments. Base editing outcomes were analyzed by **c**, NGS (non-treated cells had <0.05% base edits; data not shown) two days after the final dose, and **d**, flow cytometry was performed three days after the last dose to detect knockout of CCR5 surface expression. n=3 biological replicates from distinct human donors for the one-dose experiment; n=2 for the two-dose and three-dose experiments. Bars represent the mean; error bars represent S.E.M. *P*-values are from two-tailed Welch's unpaired *t*-tests.

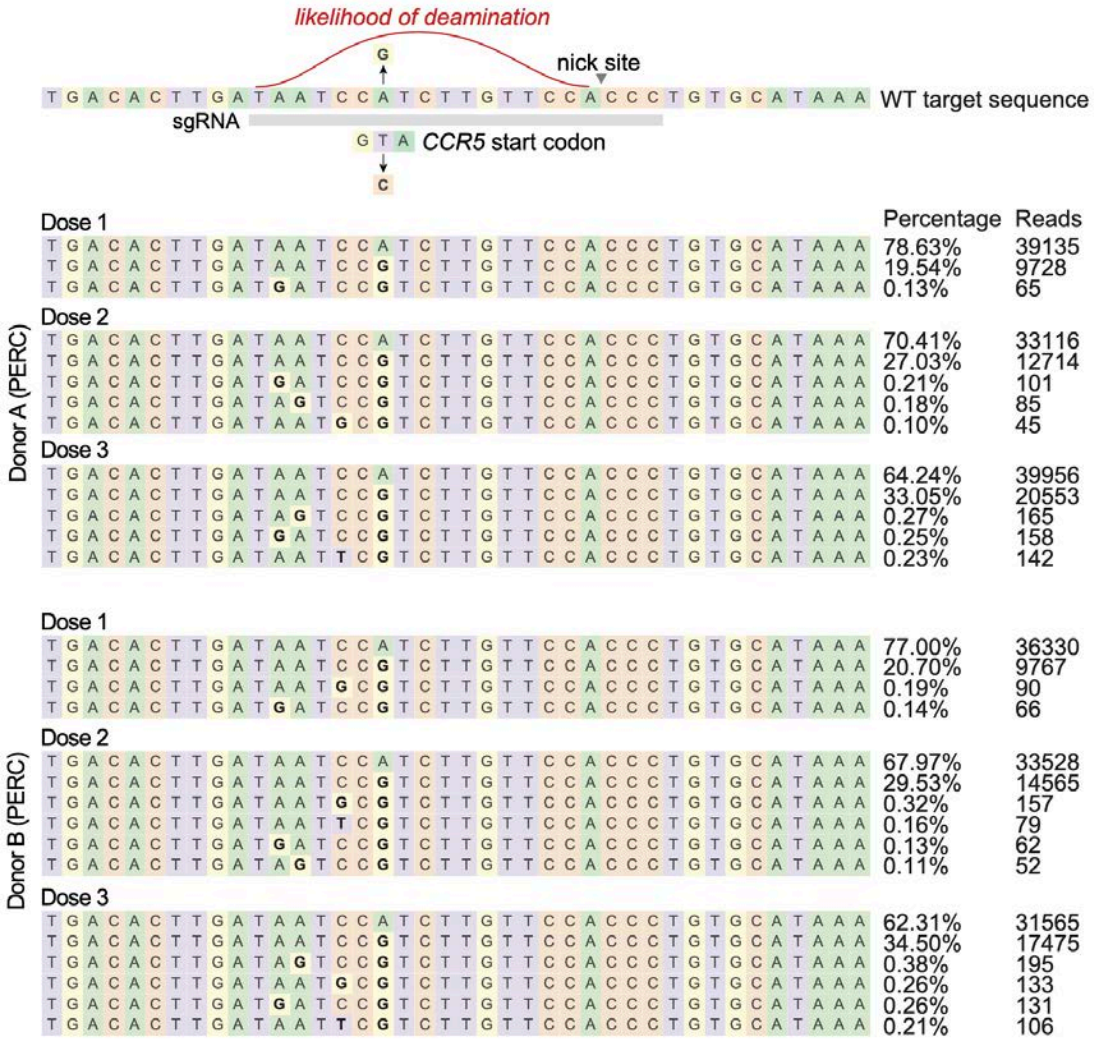


**Supplementary Fig. 11 |** Base editing outcomes following PERC. Allele plots showing NGS-based sequencing reads from T cells that received ABE8e-Cas9-NG RNP targeting the start codon of *CCR5*. RNP was delivered up to three times using PERC, and the reads resulting from each dosing strategy are reported. Because 0.1% is the approximate practical limit of detection for our analysis, only reads with frequency ≥0.1% are shown. Related to **Supplementary Fig. 10, 12**. The intended A→G conversion is outlined in red, and these reads contributed to the editing efficiency reported in **Supplementary Fig. 10**. Unintended C→T and C→G conversions were detected at the two C nucleotides 5′ (left) of the targeted A. These unintended conversions were detected only in reads that also contained the intended A→G conversion that ablates the *CCR5* start codon.

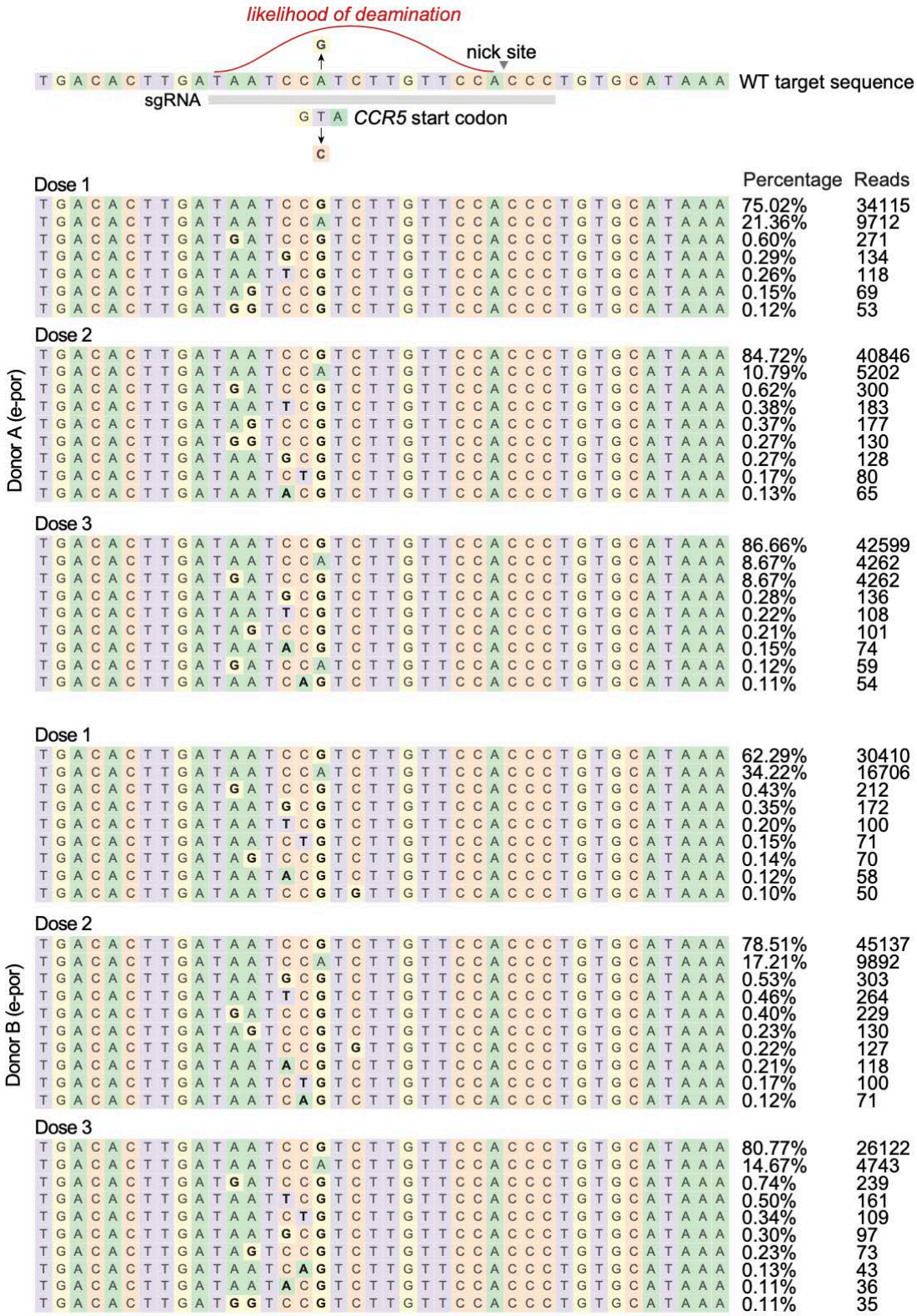


**Supplementary Fig. 12 |** Base editing outcomes following electroporation. Allele plots showing NGS-based sequencing reads from T cells that received ABE8e-Cas9-NG RNP targeting the start codon of *CCR5*. RNP was delivered up to three times using electroporation, and the reads resulting from each dosing strategy are reported. Because 0.1% is the approximate practical limit of detection for our analysis, only reads with frequency ≥0.1% are shown. Related to **Supplementary Fig. 10, 11**. The intended A→G conversion is outlined in red, and these reads contributed to the editing efficiency reported in **Supplementary Fig. 10**. Unintended C→T and C→G conversions were detected at the two C nucleotides 5′ (left) of the targeted A. These unintended conversions were detected only in reads that also contained the intended A→G conversion that ablates the *CCR5* start codon.

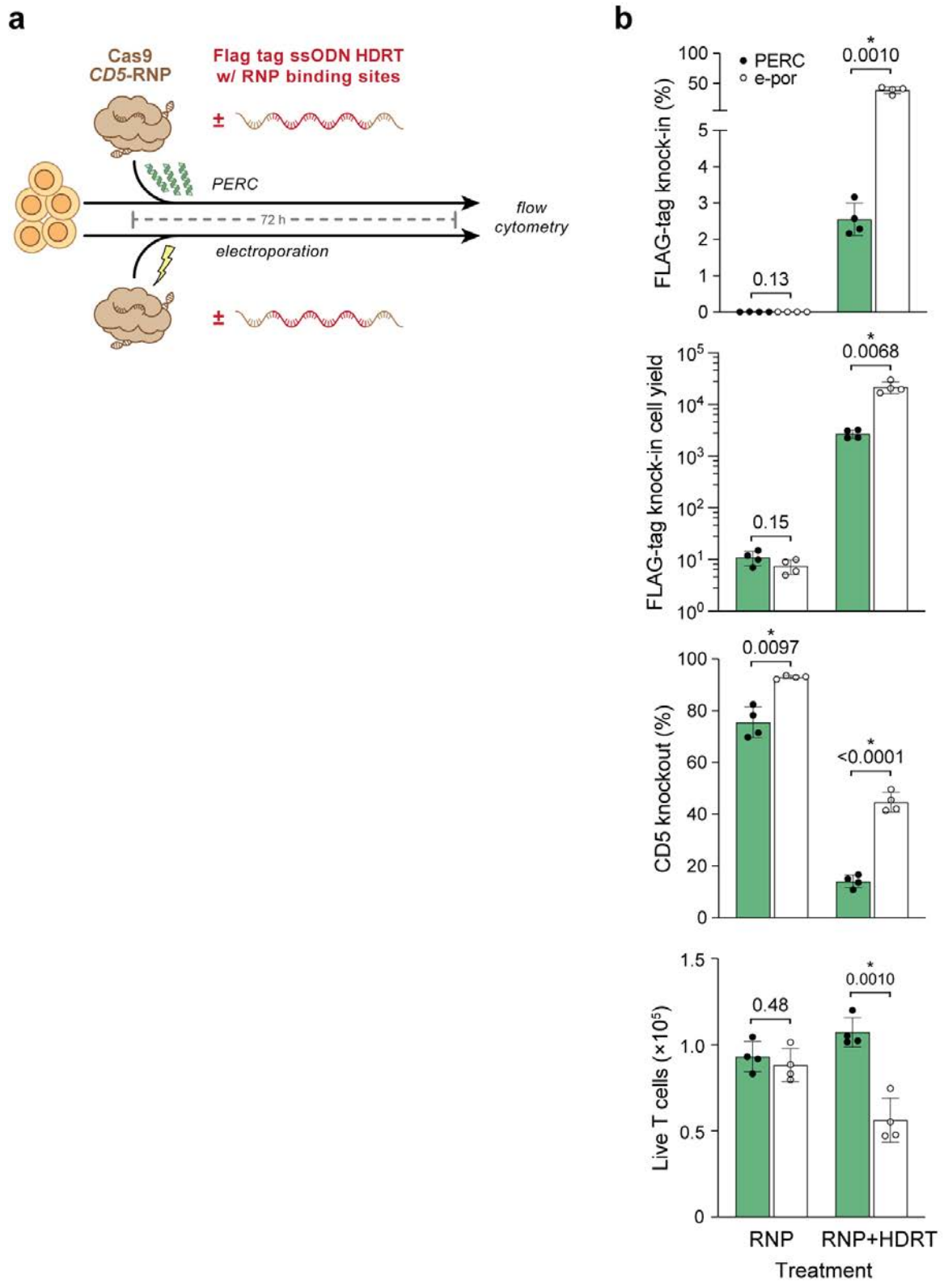


**Supplementary Fig. 13 |** Comparison of PERC and electroporation with an ssODN HDRT. **a**, Schematic representing the experimental protocol for delivery of Cas9 *CD5*-RNP with or without DNA HDRT for FLAG-tag knock-in, via either PERC using A5K (30 µM) or electroporation, in $CD4^+$ T cells. **b**, Knockout and knock-in editing were assessed by flow cytometry. Results are presented as knock-in frequency, edited cell yield ($FLAG\text{-}tag^+$), knockout frequency ($CD5^-$), and total number of live cells in each treatment. n=4 biological replicates from distinct human donors. Bars represent the mean, and error bars represent ± S.D. *P*-values are from two-tailed Welch's unpaired *t*-tests.

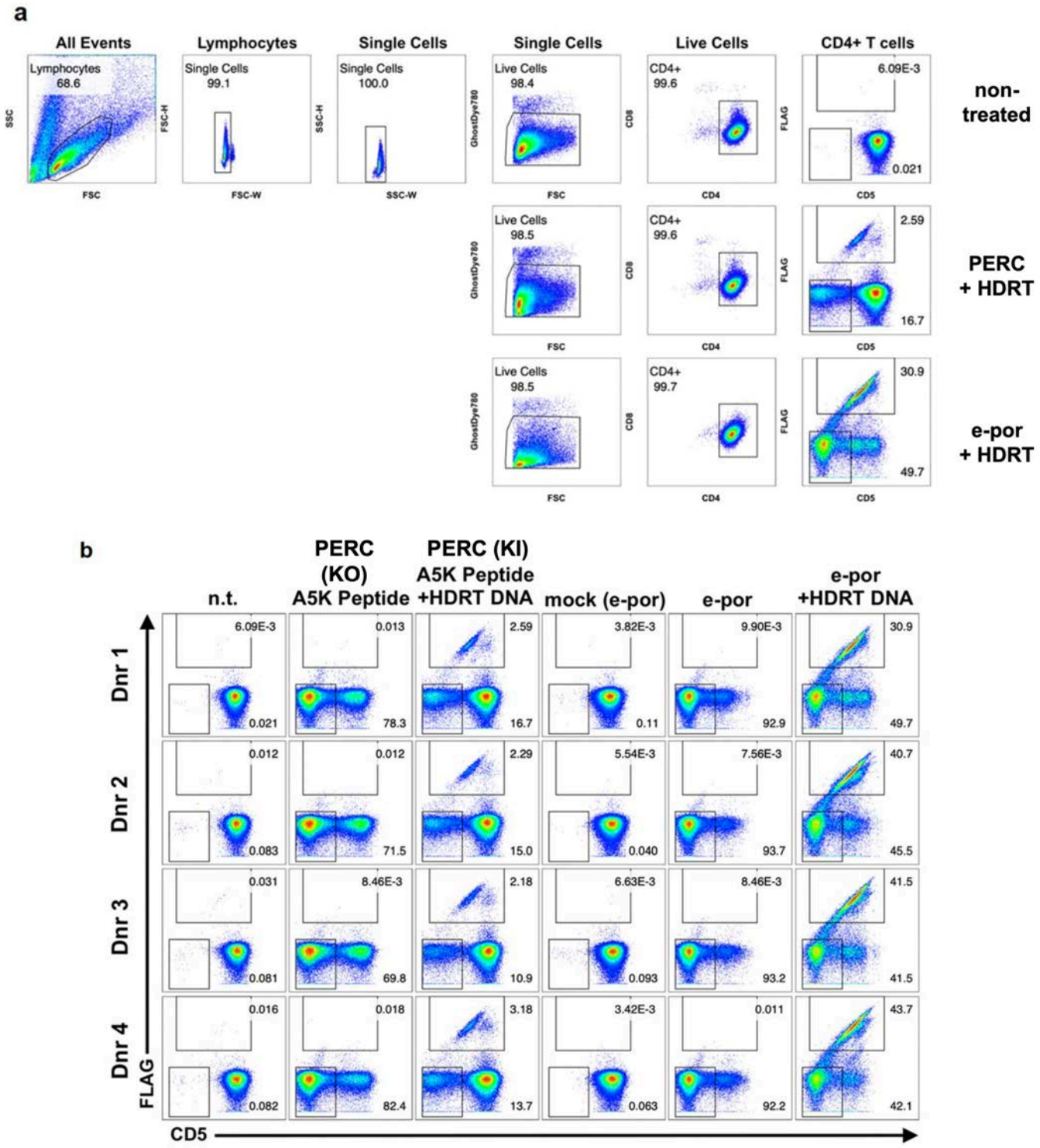


**Supplementary Fig. 14 | a,b**, Flow cytometry gating to assess CD5 knockout and FLAG-tag knock-in in CD4⁺ T cells. Cas9 *CD5*-RNP was delivered via PERC or electroporation, with or without DNA HDRT for FLAG-tag knock-in.

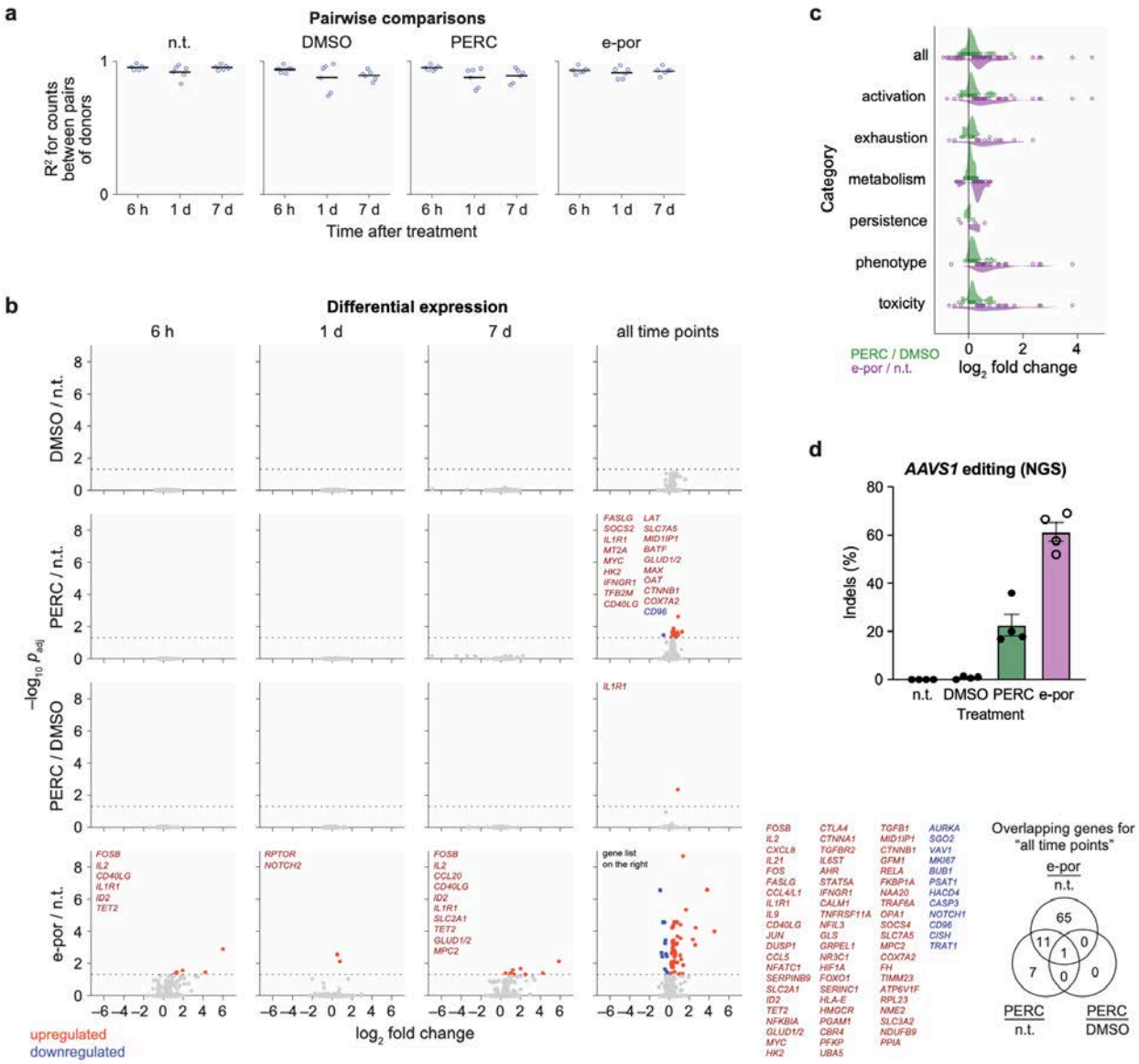


**Supplementary Fig. 15 |** Gene expression analysis. **a**, Donor-to-donor correlations ($R^2$) in gene expression. For n=4 biological replicates from distinct donors, there are six pairwise comparisons. **b**, The volcano plots depict gene expression fold changes and adjusted *p*-values at each time point and for all time points incorporated. Red denotes significant upregulation and blue denotes significant downregulation. The Venn diagram depicts the number of and overlap in differentially expressed genes. **c**, Comparison of fold changes across gene categories, considering the n = 77 genes that are differentially expressed in either PERC/DMSO or e-por/n.t. **d**, Indel percentages for each condition, as determined by NGS.

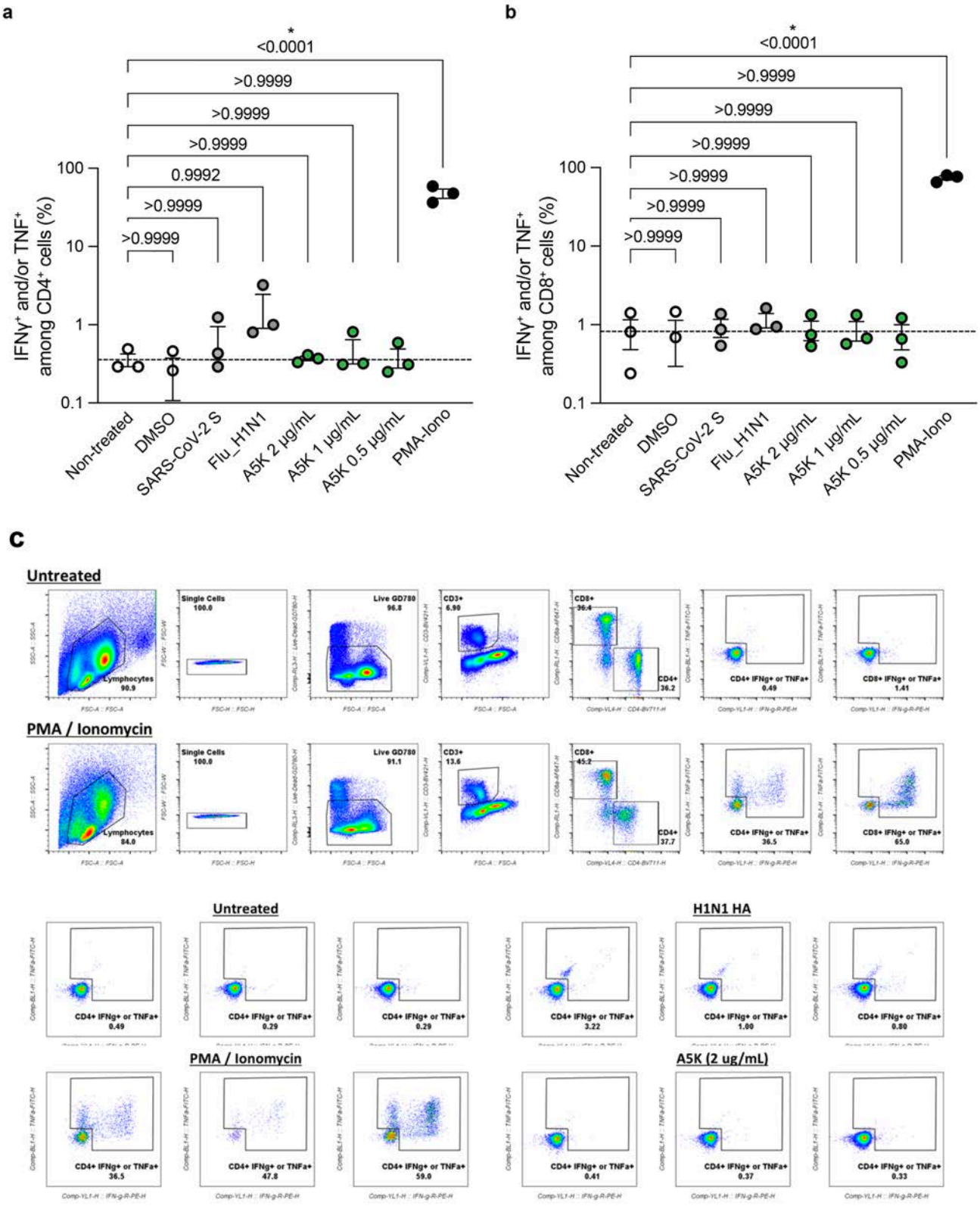


**Supplementary Fig. 16 |** A5K peptide does not promote an antigen-specific T cell response. PBMCs were isolated and cultured in the presence of either A5K peptide, peptide pools derived from SARS-CoV-2 or influenza virus H1N1, or controls as indicated. **a**, $CD4^+$ T cell and **b**, $CD8^+$ T cell subsets were assessed for production of IFN-γ or TNF. *P*-values are from an ANOVA and Holm-Šidák multiple comparisons test. **c**, Intracellular staining and flow cytometry with representative flow analysis gating. n=3 biological replicates from distinct human donors. Bars represent the mean, and error bars represent ± S.E.M.

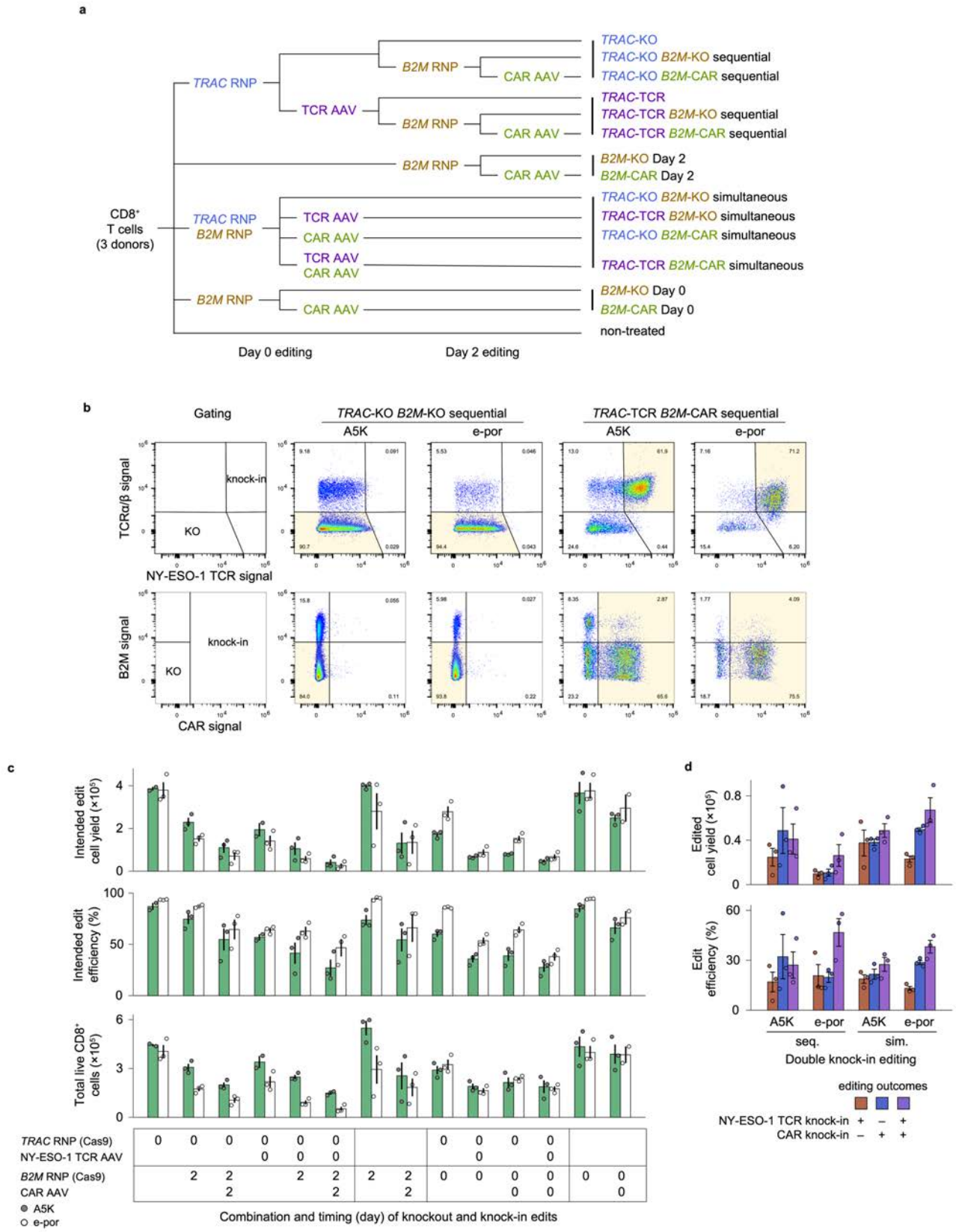


**Supplementary Fig. 17 |** Sequential vs. simultaneous editing (related to **Fig. 1d** and **Fig. 3a,b**). **a**, Experiment schematic. **b**, Gating on representative samples. **c,d**, Editing outcomes. Dotted boxes in **c** indicate conditions that were investigated further in **Fig. 3e** (translocation analysis). CD8⁺ T cell editing involved Cas9 *TRAC*-RNP & NY-ESO-1 TCR AAV and Cas9 *B2M*-RNP & CAR AAV. Non-treated cells express TCRα/β and B2M. Double knockout cells are defined as TCRα/β⁻ NY-ESO-1 TCR⁻ B2M⁻ CAR⁻. Double knock-in cells are defined as TCRα/β⁺ NY-ESO-1 TCR⁺ CAR⁺. n=3 biological replicates from distinct human donors. Bars represent the mean, and error bars represent ± S.E.M.

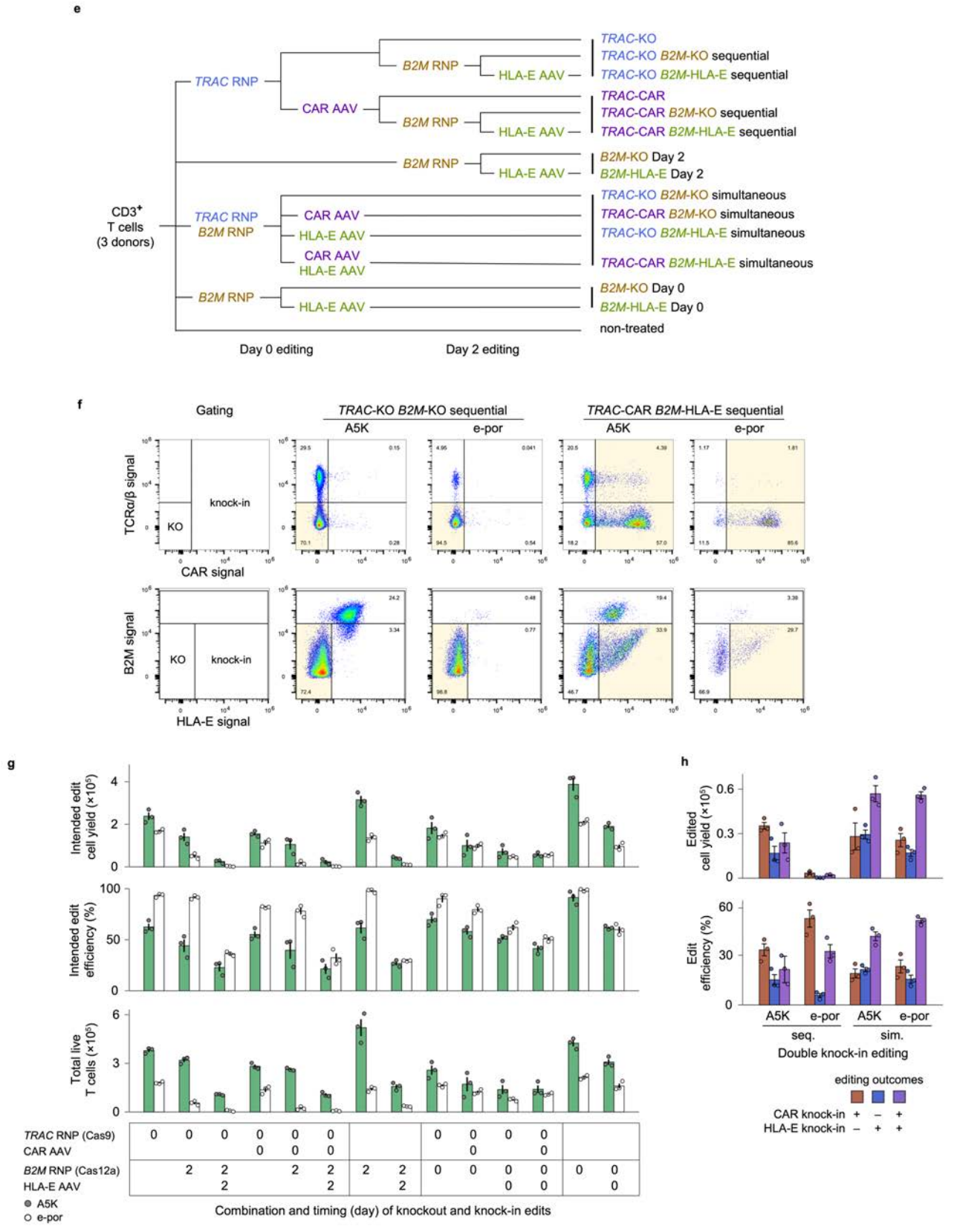


**Supplementary Fig. 18 |** Sequential vs. simultaneous editing (related to **Fig. 1d** and **Fig. 3c,d**). **a**, Experiment schematic. **b**, Gating on representative samples. **c,d**, Editing outcomes. $CD3^+$ T cell editing involved Cas9 *TRAC*-RNP & CAR AAV and Cas12a *B2M*-RNP & HLA-E AAV. Non-treated cells express TCRα/β, B2M at a high level, and HLA-E at a low level. Double knockout cells are defined as $TCR\alpha/\beta^-$ $CAR^-$ $B2M^-$ $HLA\text{-}E^-$. Double knock-in cells are defined as $CAR^+$ $B2M^{lo}$ $HLA\text{-}E^+$. Compared to non-treated cells, cells with HLA-E knock-in express HLA-E at a high level. n=3 biological replicates from distinct human donors. Bars represent the mean, and error bars represent ± S.E.M.

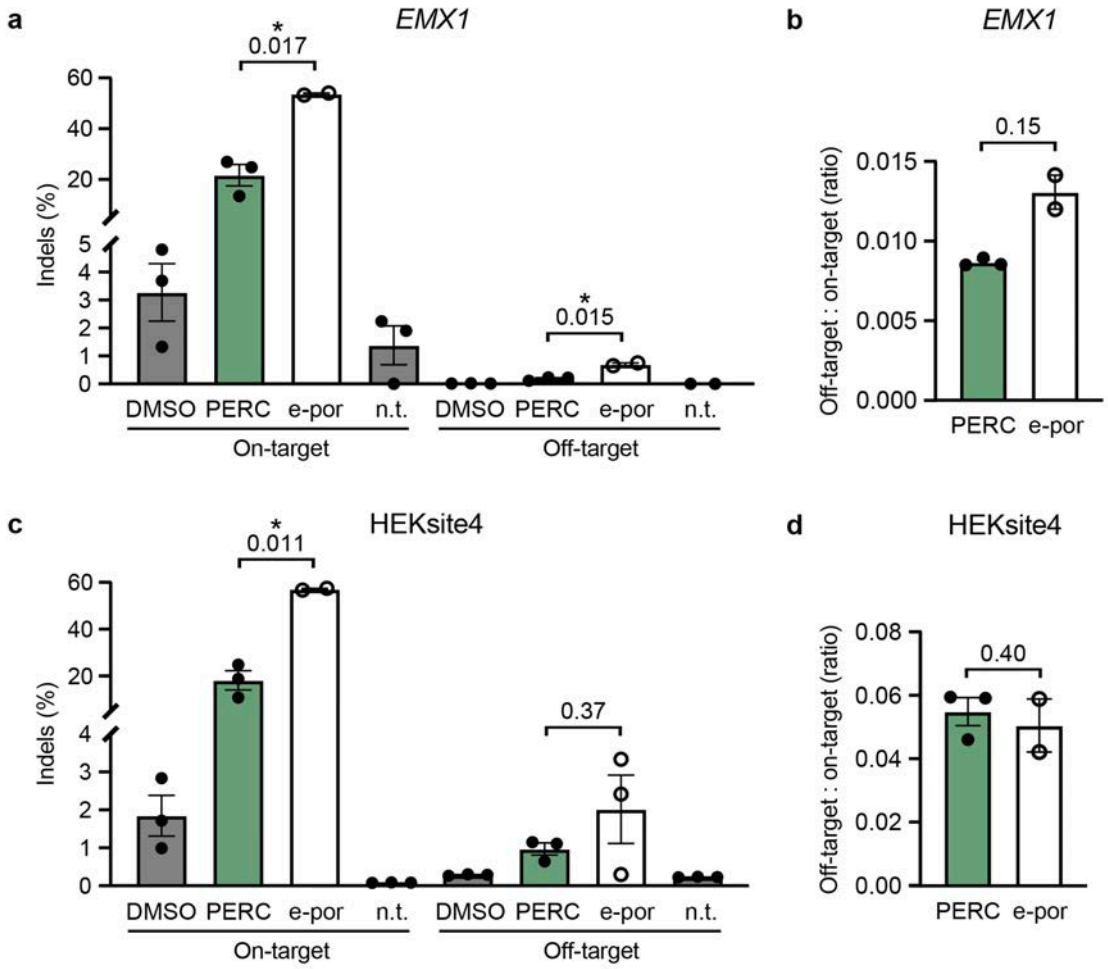


**Supplementary Fig. 19 |** Analysis of off-target effects. On-target and off-target editing efficiencies were assessed by amplicon-based NGS in CD4⁺ T cells treated with Cas9 RNP targeting two loci, **a,b**, *EMX1* and **c,d,** HEKsite4. Bars represent the mean, and error bars represent ± S.E.M. *P*-values are from two-tailed Welch's unpaired *t*-tests. n=3 biological replicates from distinct human donors. Guide RNA sequences are listed in **Supplementary Table 2**.

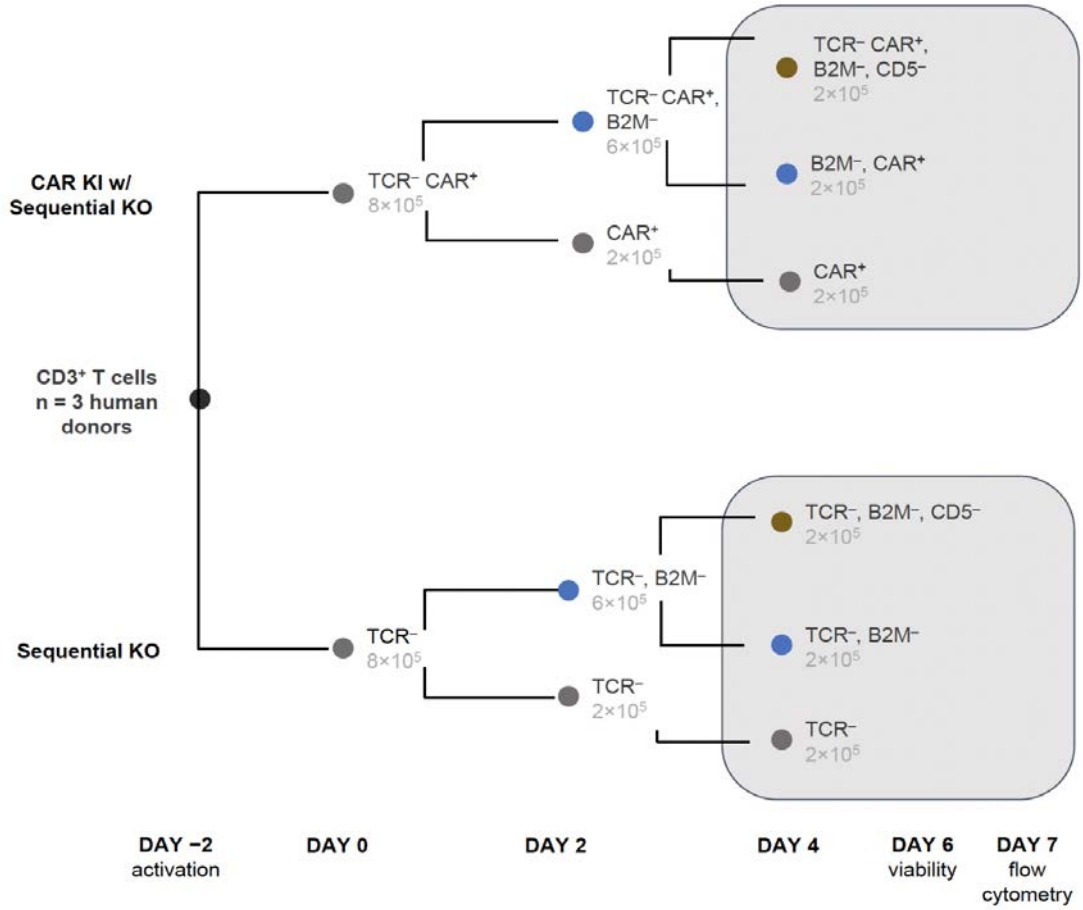


**Supplementary Fig. 20 |** Schematic of sequential editing of three loci in CD3+ T cells. Upper branch: Cas9 *TRAC*-RNP and CAR AAV on Day 0, Cas9 *B2M*-RNP on Day 2, and Cas9 *CD5*-RNP on Day 4 (related to **Fig. 4b**). Lower branch: Cas9 RNPs without CAR AAV (related to **Fig. 4c**). Cell numbers in each condition were scaled up if cells needed to be subsequently split for sequential editing, with the treatment appropriately scaled for the number of cells. Cell density was returned to $1\times10^6$ cells/mL at each branch point. To compare edited cell counts between conditions at different branch points, data were normalized to assume the same starting cell number. Flow cytometry was conducted on Day 7.

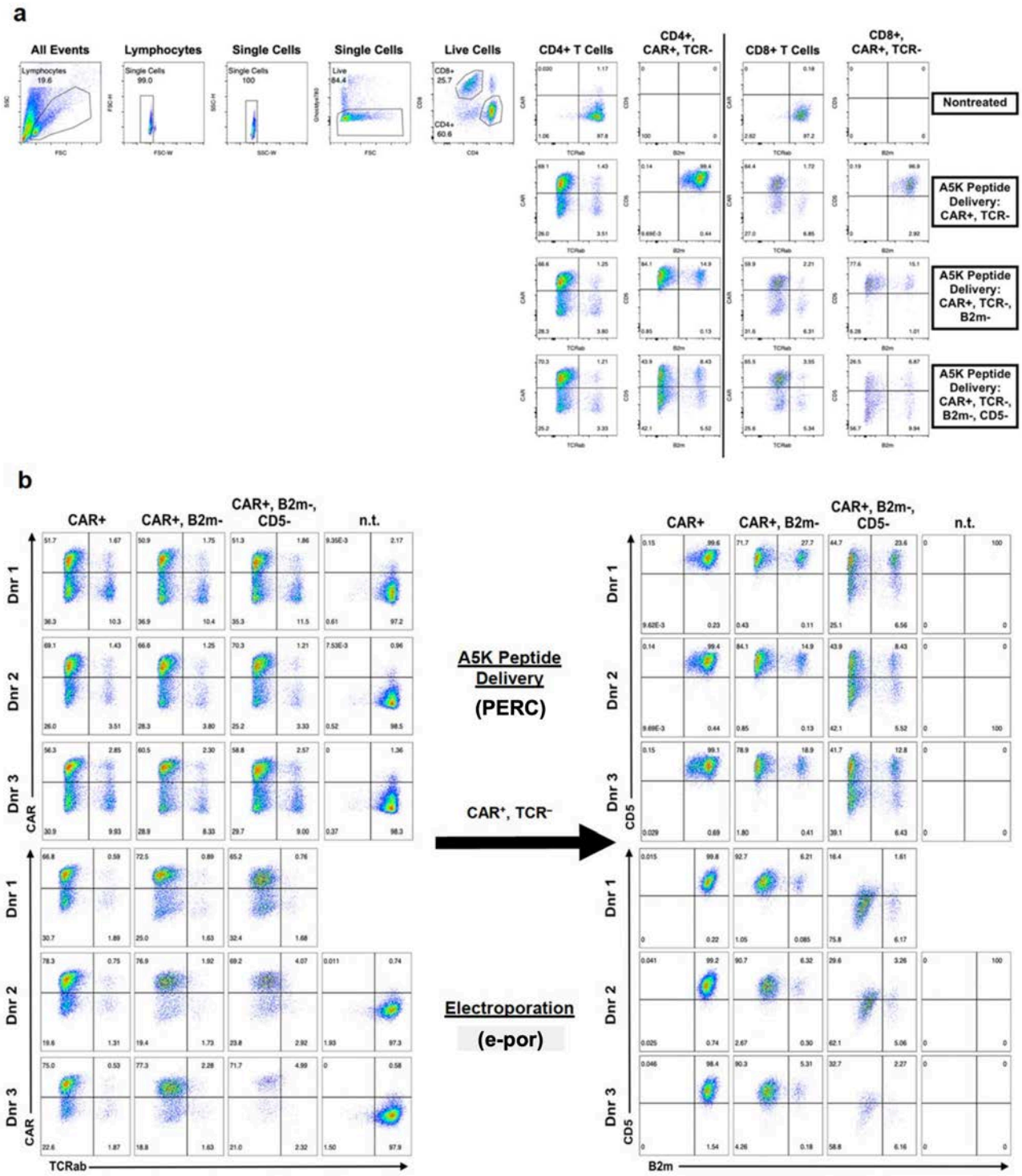


**Supplementary Fig. 21 | a**, Representative flow cytometry gating for assessing TCR surface expression following Cas9 *TRAC*-RNP delivery to and CAR AAV transduction of CD3+ T cells (related to **Fig. 4b**). **b**, Representative gating for assessing knockout of B2M and CD5 in sequentially edited CAR+ T cells (related to **Fig. 4b**).

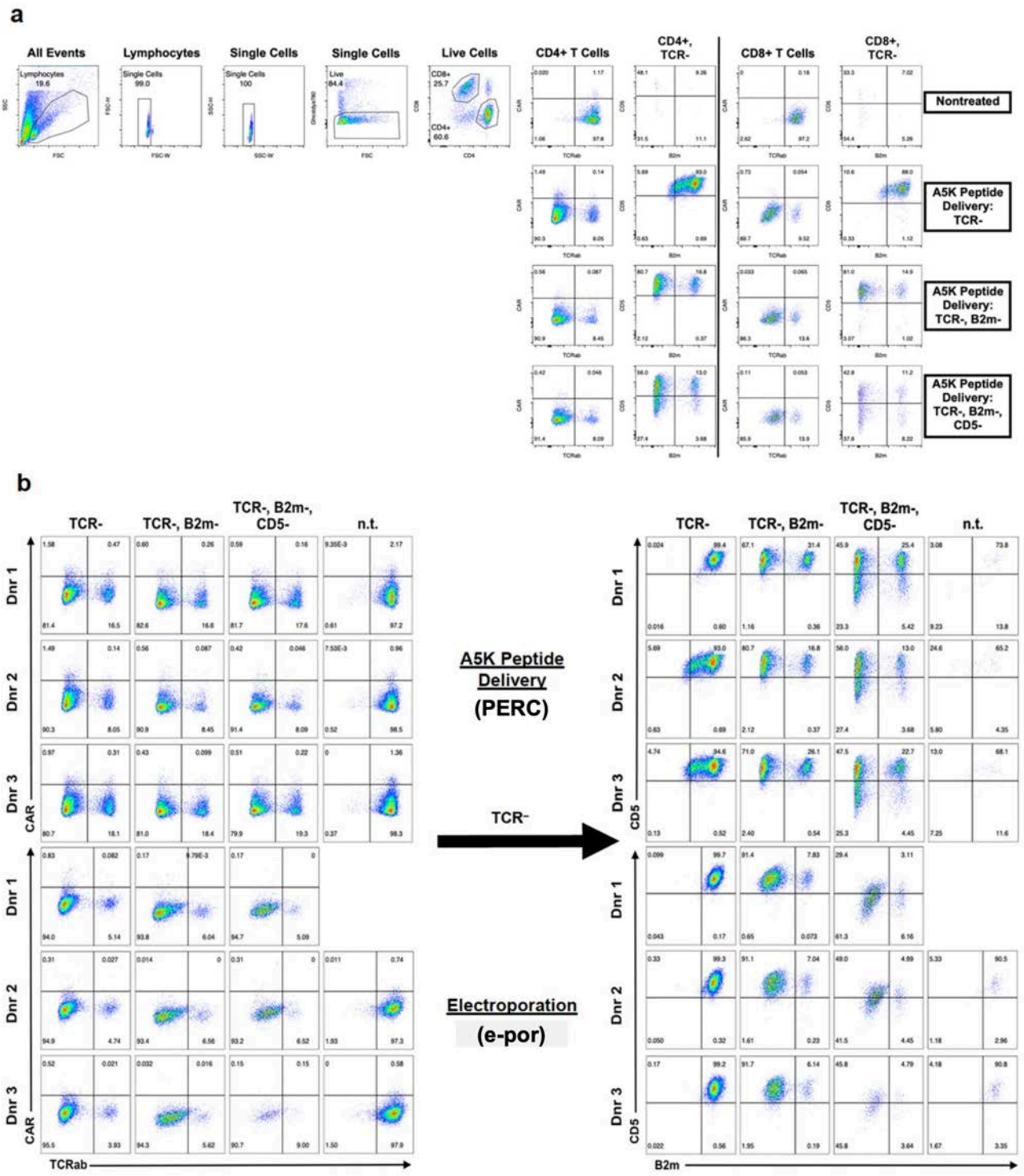


**Supplementary Fig. 22 | a**, Representative flow cytometry gating for assessing TCR surface expression following Cas9 *TRAC*-RNP delivery to CD3⁺ T cells (related to **Fig. 4c**). **b**, Representative gating for assessing knockout of B2M and CD5 in sequentially edited T cells (related to **Fig. 4c**).

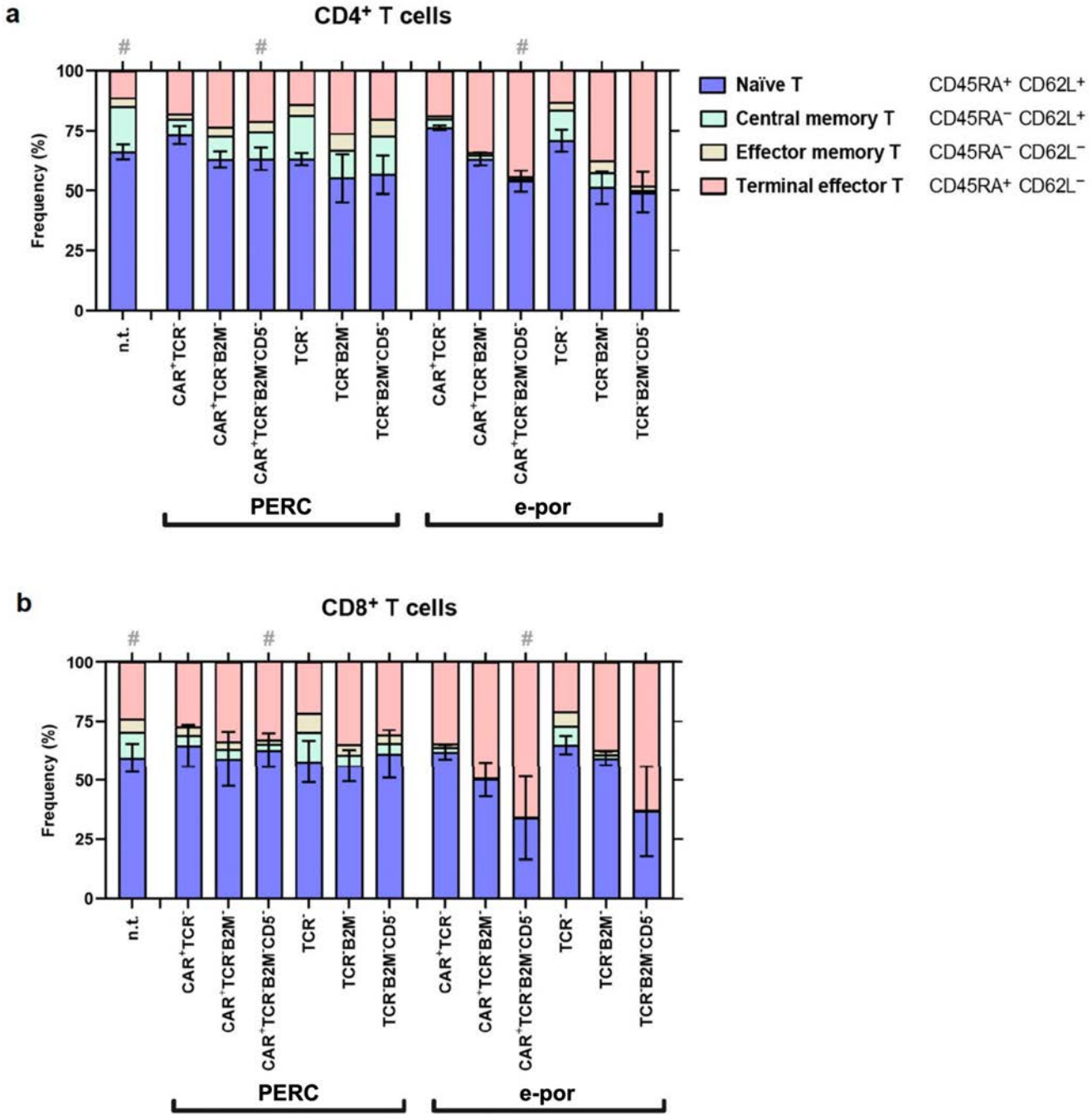


**Supplementary Fig. 23 | a,b**, Flow cytometry assessment of CD62L/CD45RA phenotypes in $CD4^+$ and $CD8^+$ T cells. For each sequential editing treatment via PERC or electroporation (outlined in **Supplementary Fig. 20**), phenotypes were assessed independent of editing outcome. Representative flow cytometry gating shown in **Supplementary Fig. 26**. "#" indicates that data are also represented in pie charts in **Fig. 4d**. Bars represent a mean of n=3 biological replicates from distinct human donors. Error bars are displayed for the naïve populations and represent S.E.M.

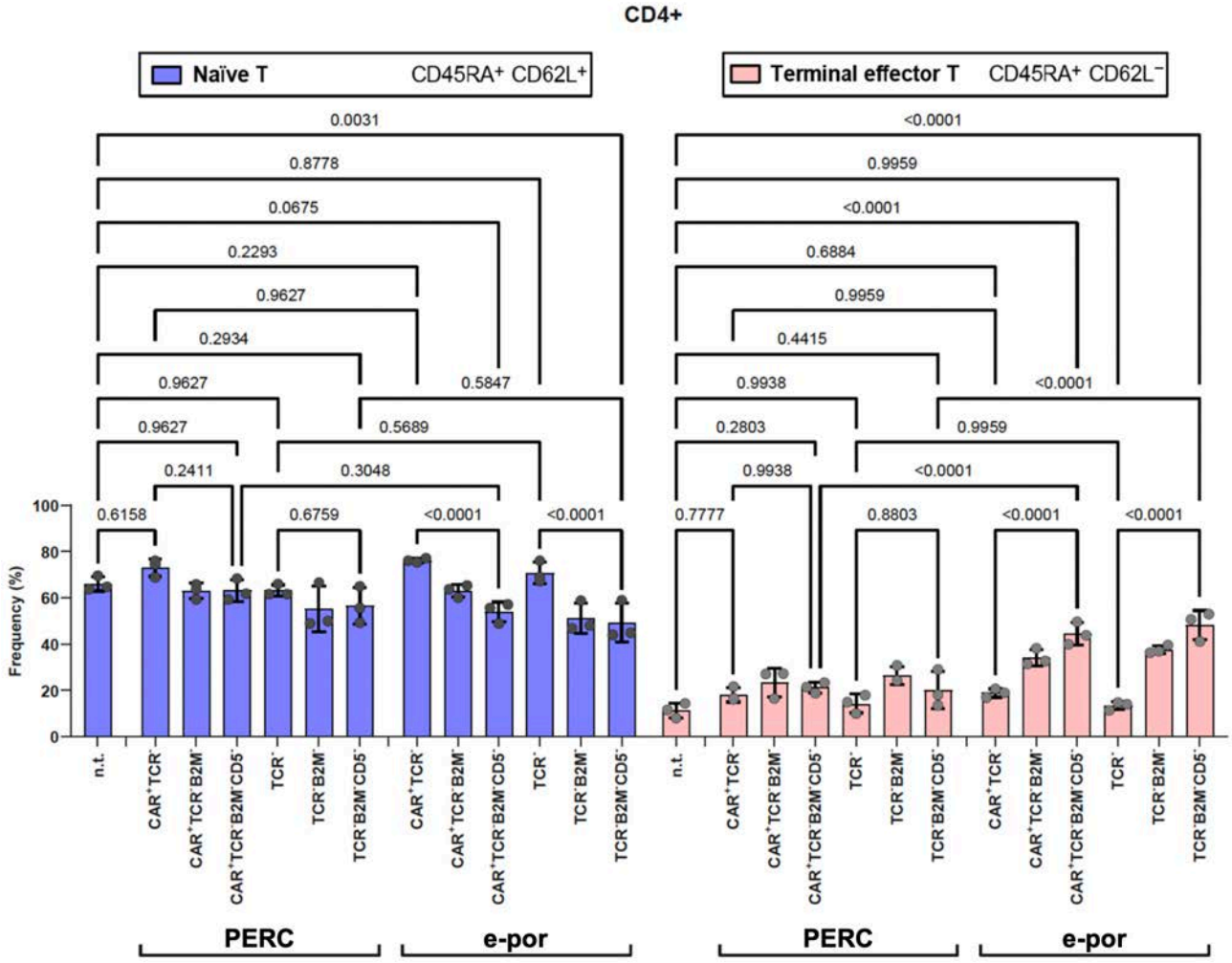


**Supplementary Fig. 24 |** Comparison of phenotypes in CD4⁺ T cells. Proportions of naïve (CD45RA⁺ CD62L⁺) and terminal effector (CD45RA⁺ CD62⁻) CD4⁺ T cells were assessed by flow cytometry. For each sequential editing treatment via PERC or electroporation (outlined in **Supplementary Fig. 20**), phenotypes were assessed independent of editing outcome. Representative flow cytometry gating shown in **Supplementary Fig. 26**. Same data as in **Supplementary Fig. 23**. Brackets indicate each comparison between two populations with adjusted *p*-values from a two-way ANOVA with Holm-Sidak's correction method for multiple comparisons. Bars represent a mean of n=3 biological replicates from distinct human donors. Error bars represent S.E.M.

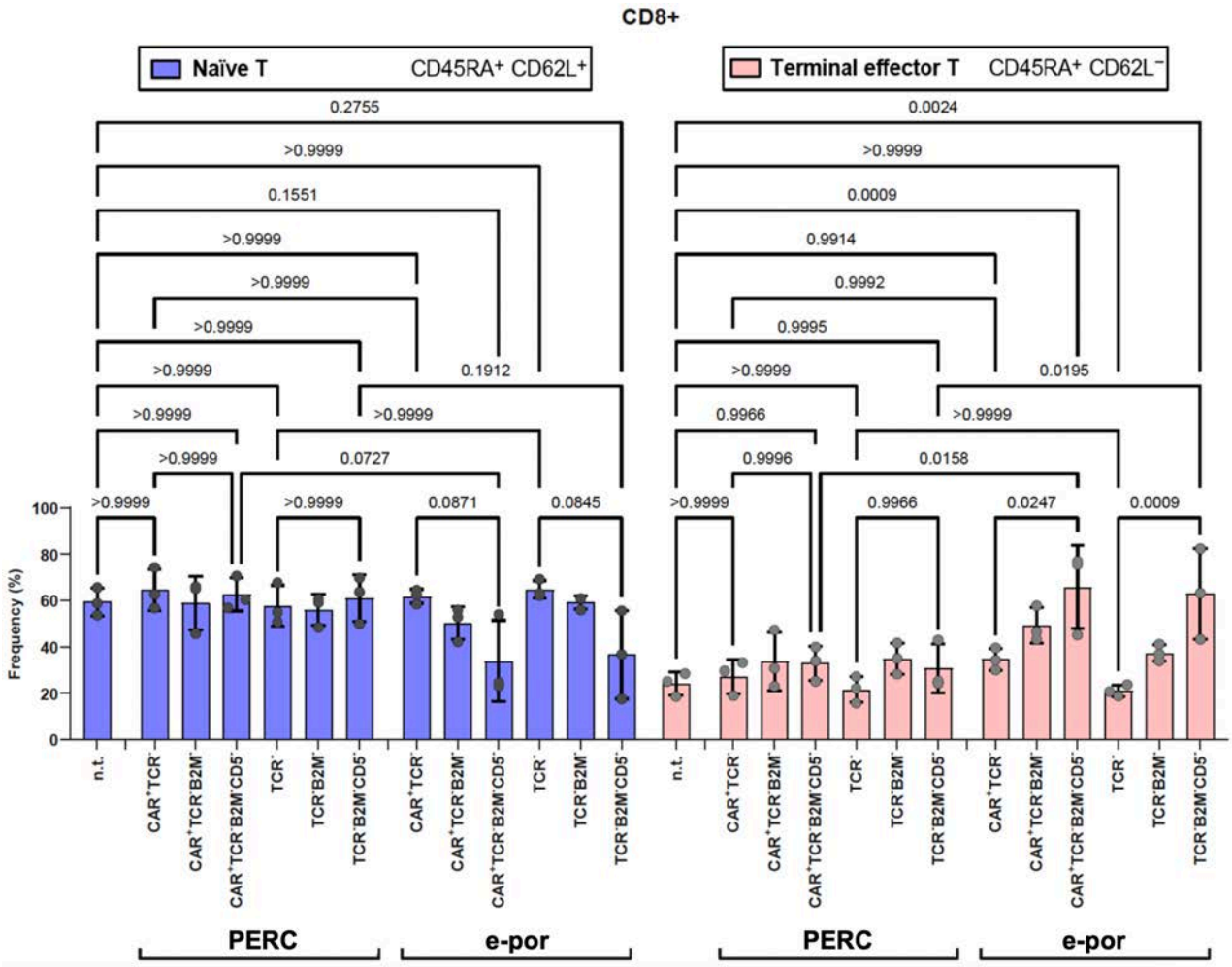


**Supplementary Fig. 25 |** Comparison of phenotypes in CD8⁺ T cells. Proportions of naïve (CD45RA⁺ CD62L⁺) and terminal effector (CD45RA⁺ CD62L⁻) CD8⁺ T cells were assessed by flow cytometry. For each sequential editing treatment via PERC or electroporation (outlined in **Supplementary Fig. 20**), phenotypes were assessed independent of editing outcome. Representative flow cytometry gating shown in **Supplementary Fig. 26**. Same data as in **Supplementary Fig. 23**. Brackets indicate each comparison between two populations with adjusted *p*-values from a two-way ANOVA with Holm-Sidak's correction method for multiple comparisons. Bars represent a mean of n=3 biological replicates from distinct human donors. Error bars represent S.E.M.

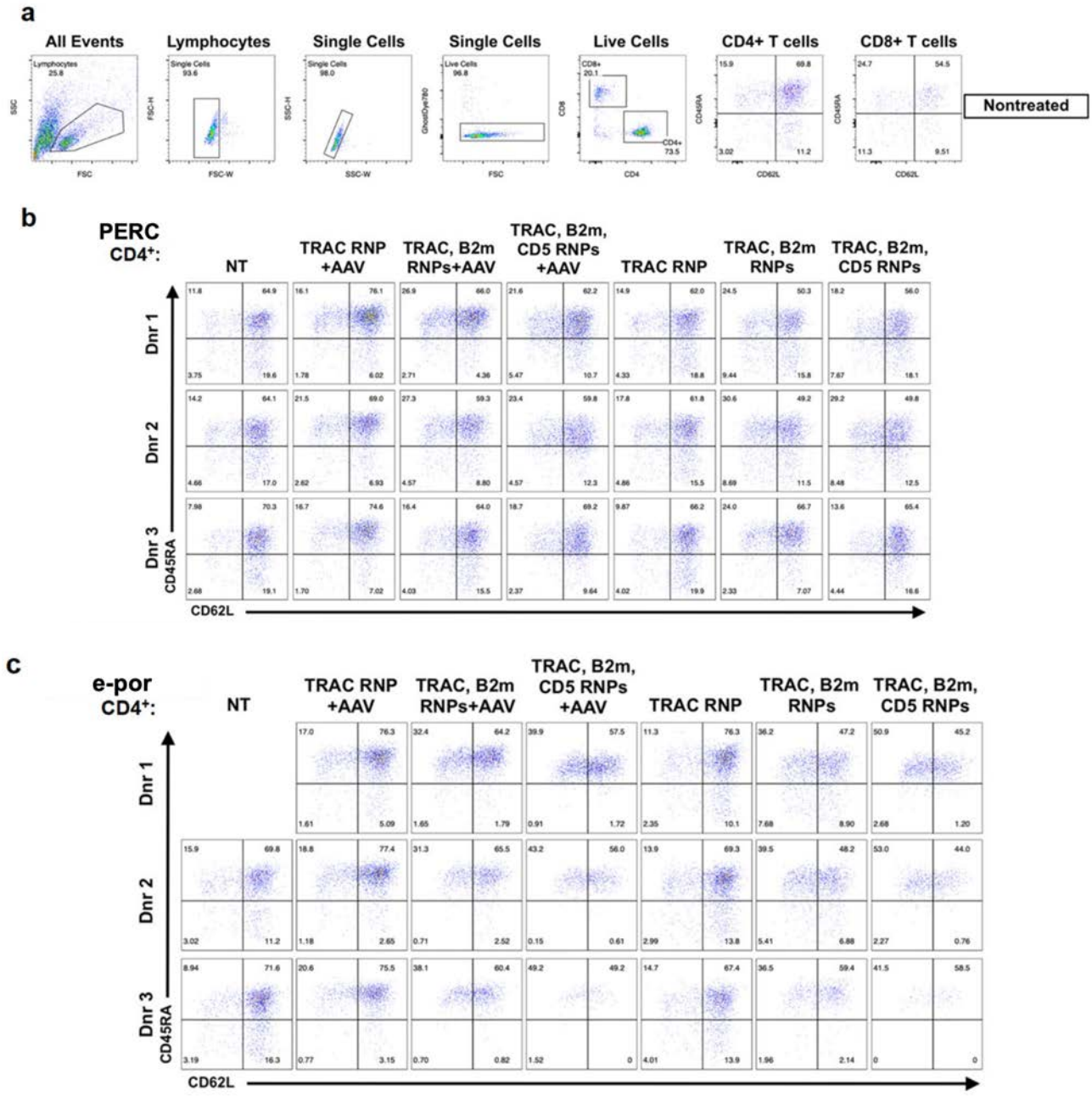


**Supplementary Fig. 26 | a–c**, Representative flow cytometry gating for assessing CD62L/CD45RA phenotypes. The conditions shown are for sequential editing via PERC or electroporation (outlined in **Supplementary Fig. 20**). Phenotypes were assessed independent of editing outcome.

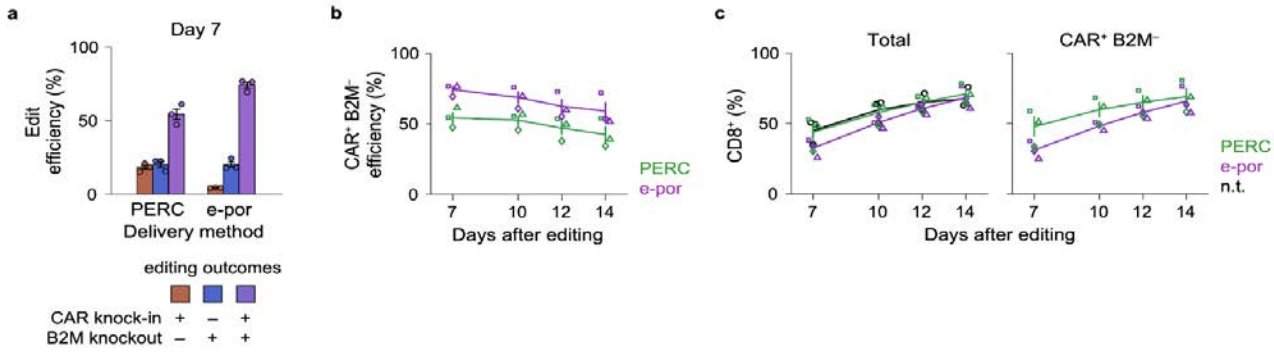


**Supplementary Fig. 27 |** T cell editing for the extended culture experiment. **a**, Percentages of cells that underwent CAR knock-in and/or B2M knockout. **b**, Percentages of edited cells over time. **c**, Percentages of $CD8^+$ cells over time, considering all cells or the $CAR^+$ subset.

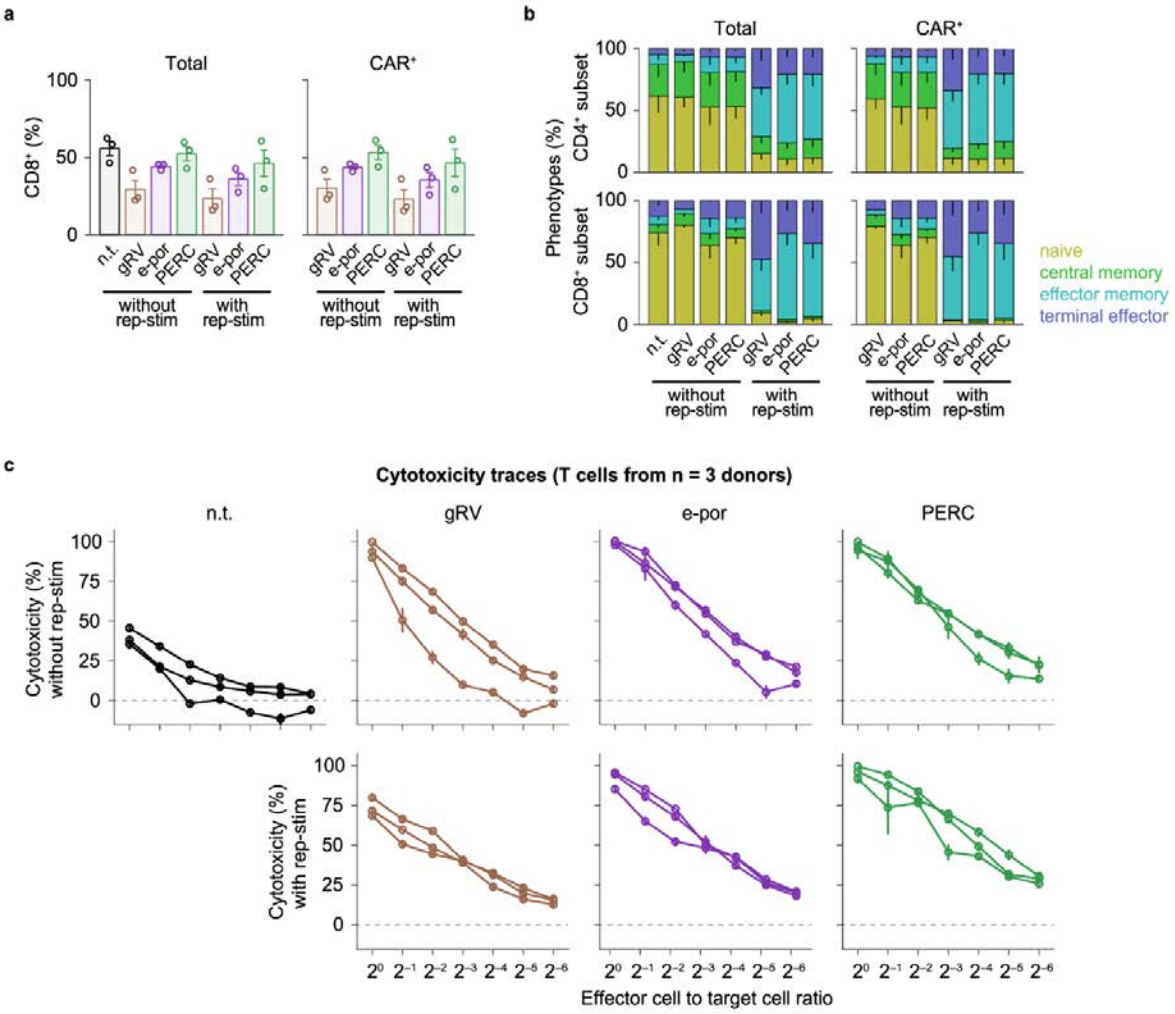


**Supplementary Fig. 28 |** T cell editing for the repetitive stimulation experiment. **a**, Percentages of CD8+ cells in each condition, considering all cells or the CAR+ subset. **b**, CD62L/CD45RA phenotypes of CD4+ and CD8+ cells, considering all cells or the CAR+ subset. **c**, Cytotoxicity traces for T cells from each of three donors (related to **Fig. 5c**). Error bars represent S.E.M from three technical replicates.

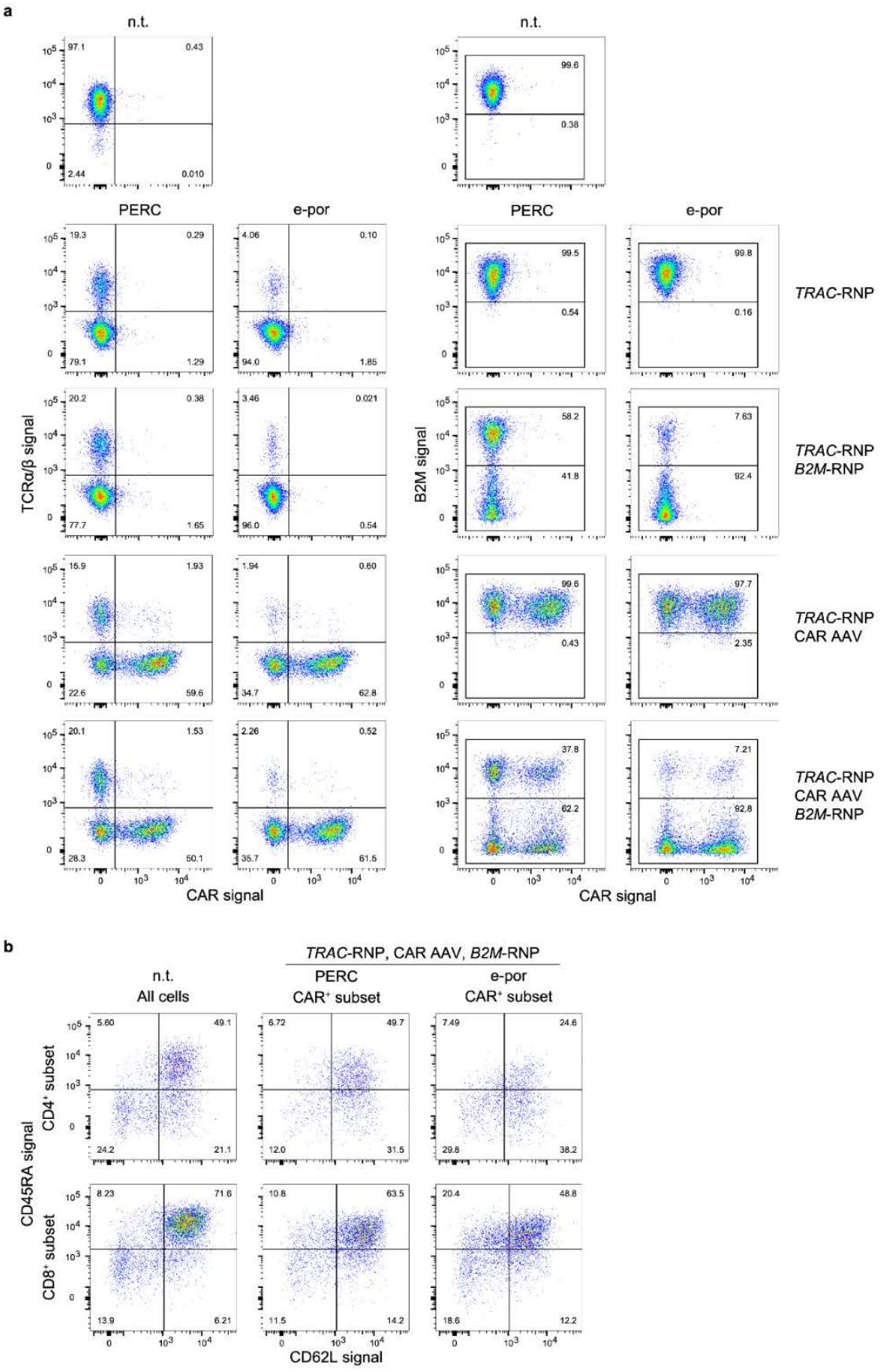


**Supplementary Fig. 29 |** T cell editing for the *in vivo* tumor challenge experiment. **a,b**, Flow cytometry characterization of editing outcomes and phenotype prior to injection. Edited cells that were injected were treated with Cas9 *TRAC*-RNP, CAR AAV, and Cas9 *B2M*-RNP.

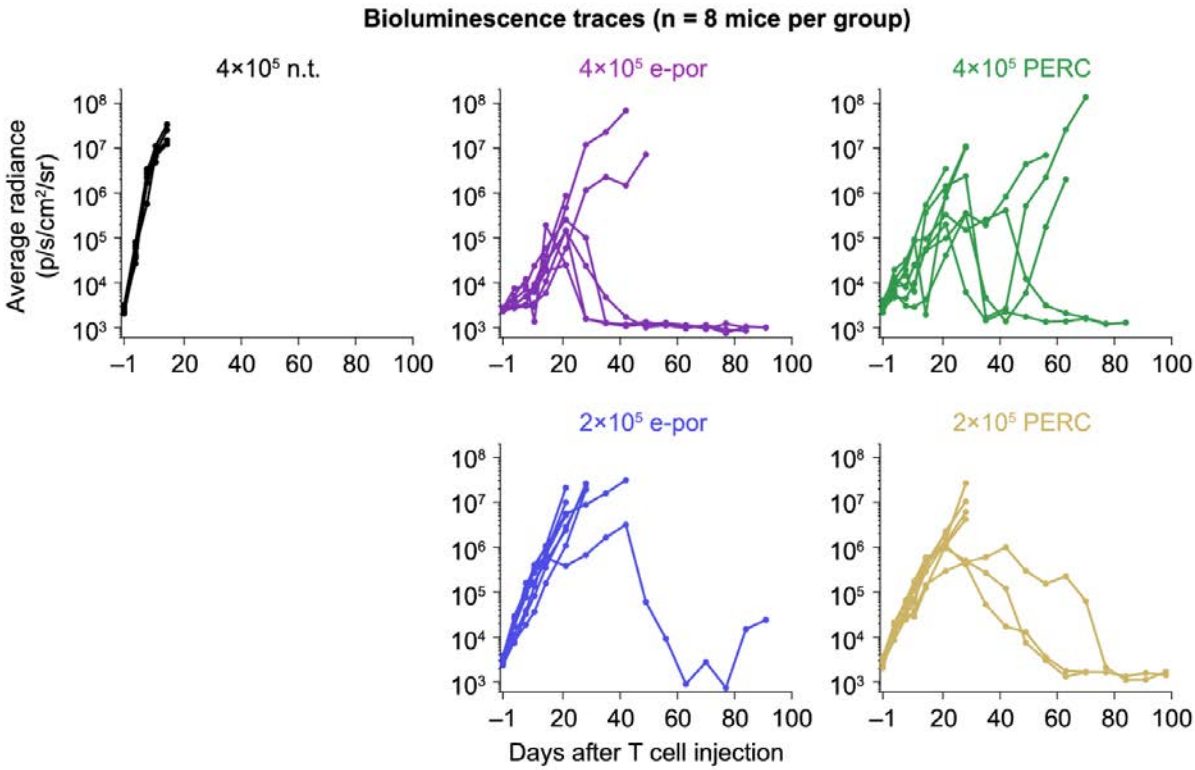


**Supplementary Fig. 30 |** Bioluminescence imaging trace for each mouse; associated with data in **Fig. 5g**.

| # | Name | Sequence |
|---|---|---|
| 1 | **E5-TAT** | GLFEAIAEFIENGWEGLIEGWYG_GRKKRRQRRR |
| 2 | E5-TAT-Cys | GLFEAIAEFIENGWEGLIEGWYG_GRKKRRQRRRC |
| 3 | Cys-E5-TAT | CGLFEAIAEFIENGWEGLIEGWYG_GRKKRRQRRR |
| 4 | E5-TAT_YGYG | GLFEAIAEFIENGWEGLIEGWYGYGRKKRRQRRR |
| 5 | E5-TAT_YGYG_R3 | GLFEAIAEFIENGWEGLIEGWYGYGRKKRRQRRRR |
| 6 | E5-TAT_YGAG | GLFEAIAEFIENGWEGLIEGWYGAGRKKRRQRRR |
| 7 | E5-TAT_YGGG | GLFEAIAEFIENGWEGLIEGWYGGGRKKRRQRRR |
| 8 | E5-TAT_YG | GLFEAIAEFIENGWEGLIEGWY__GRKKRRQRRR |
| 9 | E5-R8Q_YGYG | GLFEAIAEFIENGWEGLIEGWYGYGRRRRRQRRR |
| 10 | E4D-TAT | GLFEAIAEFIENGWEGLIDGWYG_GRKKRRQRRR |
| 11 | **INF7-TAT** | GLFEAIEGFIENGWEGMIDGWYGYGRKKRRQRR |
| 12 | I7T-Cys | GLFEAIEGFIENGWEGMIDGWYGYGRKKRRQRRC |
| 13 | Cys-I7T | CGLFEAIEGFIENGWEGMIDGWYGYGRKKRRQRR |
| 14 | I7T_YGG | GLFEAIEGFIENGWEGMIDGWYG_GRKKRRQRR |
| 15 | H5WYG-TAT | GLFHAIAHFIHGGWHGLIHGWYGYGRKKRRQRR |
| 16 | K5WYG-TAT | GLFKAIAKFIKGGWKGLIKGWYGYGRKKRRQRR |
| 17 | E5WYG-TAT | GLFEAIAEFIEGGWEGLIEGWYGYGRKKRRQRR |
| 18 | INF7-G1R_TAT | RLFEAIEGFIENGWEGMIDGWYGYGRKKRRQRR |
| 19 | INF7-G1K_TAT | KLFEAIEGFIENGWEGMIDGWYGYGRKKRRQRR |
| 20 | INF7-L2F_TAT | GFFEAIEGFIENGWEGMIDGWYGYGRKKRRQRR |
| 21 | INF7-E4G_TAT | GLFGAIEGFIENGWEGMIDGWYGYGRKKRRQRR |
| 22 | **INF7-A5K_TAT** | GLFEKIEGFIENGWEGMIDGWYGYGRKKRRQRR |
| 23 | INF7-E7W_TAT | GLFEAIWGFIENGWEGMIDGWYGYGRKKRRQRR |
| 24 | INF7-G8E_TAT | GLFEAIEEFIENGWEGMIDGWYGYGRKKRRQRR |
| 25 | INF7-F9L_TAT | GLFEAIEGLIENGWEGMIDGWYGYGRKKRRQRR |
| 26 | INF7-E11W_TAT | GLFEAIEGFIWNGWEGMIDGWYGYGRKKRRQRR |
| 27 | INF7-W14E_TAT | GLFEAIEGFIENGEEGMIDGWYGYGRKKRRQRR |
| 28 | INF7-E15R_TAT | GLFEAIEGFIENGWRGMIDGWYGYGRKKRRQRR |
| 29 | INF7-G16A_TAT | GLFEAIEGFIENGWEAMIDGWYGYGRKKRRQRR |
| 30 | INF7-G20L_TAT | GLFEAIEGFIENGWEGMIDLWYGYGRKKRRQRR |
| 31 | INF7-Y22N_TAT | GLFEAIEGFIENGWEGMIDGWNGYGRKKRRQRR |
| 32 | INF7_TAT-R33del | GLFEAIEGFIENGWEGMIDGWYGYGRKKRRQR_ |
| 33 | INF7_TAT-4RH | GLFEAIEGFIENGWEGMIDGWYGYGHKKHHQHR |
| 34 | ret-inv-INF7_TAT | rrqrrkkrgygywgdimgewgneifgeiaeflg ("D" amino acids) |
| 35 | INF7-E4G_M17L_TAT | GLFGAIEGFIENGWEGLIDGWYGYGRKKRRQRR |
| 36 | INF7-G1R_E7W_TAT-Y24G_R26G | RLFEAIWGFIENGWEGMIDGWYGGGGYGRKKRRQRR |
| 37 | E5-R8Q | GLFEAIAEFIENGWEGLIEGWYG_GRRRRRQRRR |

**Supplementary Table 1 |** Peptides screened in **Supplementary Fig. 1**. Highlighted peptides have corresponding colored bars in **Supplementary Fig. 1** and were also compared as part of **Fig. 1c**. Amino acid differences (from "founder" peptides, #1 or #11) are indicated in red. The retro/inverse form of INF7-TAT (peptide #34) is a reversed peptide sequence and used non-canonical D-amino acids.

| Gene target or gRNA name | Spacer sequence [PAM] | Enzyme | Cell type |
|---|---|---|---|
| *AAVS1* | GGGGCCACTAGGGACAGGAT[TGG] | SpCas9 | T cells |
| *B2M* | GAGTAGCGCGAGCACAGCTA[AGG] | SpCas9 (for KO) | T cells |
| *B2M* | GGCCACGGAGCGAGACATCT[CGG] | SpCas9 (for KI) | T cells |
| *B2M* | [TTTC]AGTGGGGGTGAATTCAGTGT | AsCas12a Ultra | T cells |
| *CD5* | CAGTCGCTTCCTGCCTCGGA[CGG] | SpCas9 | T cells |
| *CD45* | AGTACATGAATTATGAGATA[TGG] | SpCas9 | B cells, NK cells |
| CCR5off-1 | TAATCCATCTTGTTCCACCC[TGT] | ABE8e-NG-SpCas9 | T cells |
| *EMX1* | GAGTCCGAGCAGAAGAAGAA[GGG] | SpCas9 | T cells |
| HEKsite4 | GGCACTGCGGCTGGAGGTGG[GGG] | SpCas9 | T cells |
| *TRAC* | CAGGGTTCTGGATATCTGT[GGG] | SpCas9 | T cells |
| *TRAC* | [TTTA]GAGTCTCTCAGCTGGTACAC | AsCas12a Ultra | T cells |

**Supplementary Table 2 |** Guide RNAs used.

| Target | Fluorophore | Dilution | Manufacturer | Clone | Catalog # |
|---|---|---|---|---|---|
| B2M | FITC | 1:200 | BioLegend | 2M2 | 316304 |
| B2M | PE | 1:200 | BioLegend | 2M2 | 316306 |
| CAR (scFv) | AF647 | 1:100 | Jackson ImmunoResearch | polyclonal | 115-606-072 |
| CCR5 | AF647 | 1:10 | BioLegend | HEK/1/85a | 313712 |
| CD19 | APC | 1:50 | BioLegend | HIB19 | 302211 |
| CD3ε | BV421 | 1:50 | BioLegend | UCHT1 | 300434 |
| CD3ε | FITC | 1:300 | BioLegend | UCHT1 | 300405 |
| CD3ε | PE | 1:300 | BioLegend | UCHT1 | 300407 |
| CD4 | APC | 1:300 | BioLegend | OKT4 | 317415 |
| CD4 | BUV395 | 1:200 | BD Biosciences | SK3 | 563550 |
| CD4 | BV421 | 1:300 | BioLegend | OKT4 | 317433 |
| CD4 | BV711 | 1:50 | BioLegend | SK3 | 344648 |
| CD4 | PeCy7 | 1:300 | BioLegend | OKT4 | 317413 |
| CD45 | BV421 | 1:25 | BioLegend | 2D1 | 368521 |
| CD45RA | BB515 | 1:25 | BD Biosciences | HI100 | 564552 |
| CD45RA | PerCP | 1:25 | BioLegend | HI100 | 304155 |
| CD5 | APC | 1:300 | BioLegend | UCHT2 | 300611 |
| CD5 | PE | 1:200 | BioLegend | UCHT2 | 300607 |
| CD62L | BUV395 | 1:25 | BD Biosciences | DREG-56 | 740301 |
| CD62L | BV421 | 1:25 | BD Biosciences | DREG-56 | 563862 |
| CD8 | AF647 | 1:50 | BioLegend | SK1 | 344726 |
| CD8 | BV711 | 1:300 | BioLegend | SK1 | 344733 |
| CD8 | FITC | 1:300 | BioLegend | SK1 | 344703 |
| n/a | GhostDye Red 780 | 1:1000 | Tonbo Biosciences | n/a | 13-0865-T500 |
| HLA-E | PE | 1:50 | Invitrogen | 3D12HLA-E | 12-9953-42 |
| IFN-γ | PE | 1:50 | BioLegend | 4S.B3 | 502509 |
| NY-ESO-1 TCR | PE | 1:50 | Immudex | HLA-A*02:01 SLLMWITQV dextramer | WB3247 |
| TCRα/β | BV421 | 1:50 | BioLegend | IP26 | 306721 |
| TCRα/β | PE-Cy7 | 1:50 | BioLegend | IP26 | 306720 |
| TCRα/β | PerCP-Cy5.5 | 1:50 | BioLegend | IP26 | 306723 |
| TNF | FITC | 1:50 | BioLegend | MAb11 | 502906 |
| n/a | TruStain FcX | 1:25 | BioLegend | n/a | 422301 |

**Supplementary Table 3 |** Antibodies used for flow cytometry analysis.

| Gene | Forward primer sequence | Reverse primer sequence | Probe sequence | Assay |
|---|---|---|---|---|
| AAVS1 | TTCCCAGGGCCGGTTAATGTG | TCTGCCTAACAGGAGGTGGGG | – | NGS |
| *B2M* | ATATAAGTGGAGGCGTCGCG | GAAGTCACGGAGCGAGAGAG | – | NGS |
| *CCR5* | TTTGCATTCATGGAGGGCAACTAA | GGTTGAGCAGGTAGATGTCAGT | – | NGS |
| *TRAC* | CATCACTGGCATCTGGACTCCA | CGGTGAATAGGCAGACAGAC | – | NGS |
| *EMX1* on-target | CATCTGTGCCCCTCC | GTTGCCCACCCTAGTCATTGGA | – | NGS |
| *EMX1* off-target | AATGTGCTTCAACCCATCACGGCCTA | CATCAGTGTTGGCTTTCACAAGGATGG | – | NGS |
| HEKsite4 on-target | CTGAGATCCTGTCCTTAGTTTACTG | TTTCAACCCGAACGGAGAC | – | NGS |
| HEKsite4 off-target | GCAAGGCGGGAAAAGAGAAA | CTAAGCTCTCATGCCCAGGG | – | NGS |
| 5'*B2M*-3'*TRAC* | GCTGGGCACGCGTTTAATAT | TCGGTGAATAGGCAGACAGA | CATTCCTGAAGCTGACAGCATTCGGGC | ddPCR |
| 5'*TRAC*-5'*B2M* | ATCACTGGCATCTGGACTCC | GCTGGGCACGCGTTTAATAT | CATTCCTGAAGCTGACAGCATTCGGGC | ddPCR |

**Supplementary Table 4 |** Oligonucleotides used for ddPCR or for generating amplicons that were analyzed by NGS.